www.thieme.com

SYNLETT
Accounts and Rapid Communications in Chemical Synthesis

Publishing House and Copyright:
© 2023 by
Georg Thieme Verlag KG
Rüdigerstraße 14
70469 Stuttgart
ISSN 0936-5214

Thieme

Synlett V. Iziumchenko, V. Gevorgyan Cluster Account

Recent Advances in Dual Triplet Ketone/Transition-Metal Catalysis

Valeriia Iziumchenko
Vladimir Gevorgyan*

Department of Chemistry and Biochemistry, The University of Texas at Dallas, Richardson, Texas 75080, USA
vlad@utdallas.edu

This Account is dedicated to Professor Masahiro Murakami's excellent contributions to science.

Published as part of the
Special Issue Honoring Masahiro Murakami's Contributions to Science

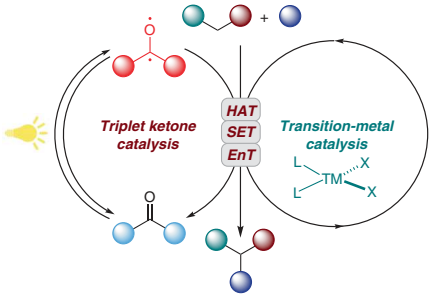

Received: 30.01.2023
Accepted after revision: 21.03.2023
Published online: 25.05.2023 (Version of Record)
DOI: 10.1055/s-0042-1751444; Art ID: ST-2023-01-0038-CA

Abstract Dual light-excited ketone/transition-metal catalysis is a rapidly developing field of photochemistry. It allows for versatile functionalizations of C–H or C–X bonds enabled by triplet ketone acting as a hydrogen-atom-abstracting agent, a single-electron acceptor, or a photosensitizer. This review summarizes recent developments of synthetically useful transformations promoted by the synergy between triplet ketone and transition-metal catalysis.

Key words dual catalysis, triplet ketone, transition-metal catalysis, photocatalysis, photosensitizer, C–H functionalization

1 Introduction

Over the last few decades, aromatic ketones have gained increased attention as inexpensive organic photocatalysts with highly tunable photophysical properties.[1] Having an extended conjugation system, aryl and diaryl carbonyls are capable of enhanced light absorption. The wavelength of the absorption maximum is often determined by electronic properties and the positions of functional groups on the ketone molecule.[2] Benzophenones undergo two electronic transitions to singlet excited states **1.2** (Scheme 1a): π–π^* transitions, usually characterized by higher energy and a higher extinction coefficient, and n–π^* transitions of lower energy and weaker absorption.[3] After a subsequent fast and efficient intersystem crossing (ISC),[4] the singlet ketone transforms into its triplet state **1.3**, which by its nature is a biradical species that is able to participate in further synthetically useful transformations (Scheme 1b).[5] Electrophilic oxygen-centered radical **1.3** is capable of hydrogen atom transfer (HAT) from substrates with relatively weak C–H bonds.[6] This process yields ketyl radical **1.4** and a substrate-originated radical. The latter, for instance, can enter another catalytic cycle to engage in a transition-metal-catalyzed reaction, while ketyl radical **1.4** can be oxidized back to the ketone to restart the triplet catalysis. An alternative fate for triplet ketone **1.3** relies on its high oxidative potential.[1d,7] Being a strong oxidant, it is able to perform a single-electron transfer (SET) with a substrate molecule.[1d,8] The resulting substrate-based radical cation, as in the previous case, can participate in further reactions. Concomitantly, the ketyl radical anion **1.5** can induce electron transfer to another reaction entity whilst being oxidized back to the ketone **1.1**.[9] Finally, one more pathway for the triplet ketone involves energy transfer (EnT) to the substrate molecule.[10] Possessing relatively long-lived excited states[11] and high triplet energy,[9,12] aryl ketones are considered to be good photosensitizers. During the energy transfer process, the triplet ketone is transformed back to its ground state **1.1**, whereas the substrate is converted into its excited state to undergo further transformations.

All the features of aryl ketones described above make them excellent partners for cooperative use with transition-metal catalysts.[13] Upon HAT, SET, or EnT, triplet ketones furnish active species for metal-catalyzed reactions transforming themselves into entities, which are easily recoverable to the ground state ketones. This review covers recent developments in triplet ketone/transition-metal dual catalysis, categorized by the mechanism of triplet ketone performance.

Georg Thieme Verlag KG, Rüdigerstraße 14, 70469 Stuttgart, Germany

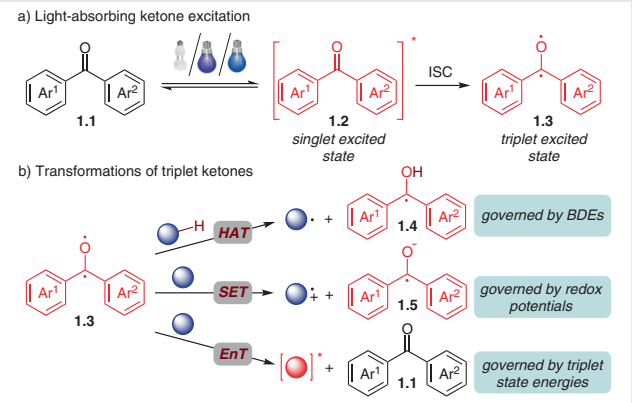

Scheme 1 Light-absorbing ketones as organic photocatalysts

2 Triplet Ketone Catalysis via Hydrogen Atom Transfer

2.1 Triplet Ketones with Nickel Catalysis

Arguably, the employment of light-excited ketones as HAT agents is the most abundant application among all types of triplet ketone catalysis. The combination of benzophenone and nickel catalysts has a long history since the discovery of photoreduction of Ni(II) precatalysts to Ni(I) complexes in the presence of aromatic ketones in H-donating solvents.[14] The formed Ni(I) complexes disproportionate into $L_nNi(II)X_2$ and catalytically active $L_nNi(0)$ species.[15]

In 2018, Martin utilized push–pull ketone **2.3** under compact fluorescent lamp (CFL) irradiation in tandem catalysis with nickel for the C(sp^3)–H arylation and alkylation of ethers, toluene, and simple cycloalkanes (Scheme 2).[16] The combination of 10 mol% of $Ni(acac)_2$, 10 mol% of ketone **2.3** (4-methoxy-4′-(trifluoromethyl)benzophenone), and 10 mol% of ligand **2.4** (5,5′-dimethyl-2,2′-bipyridine) was used to arylate tetrahydrofuran (THF), other cyclic and linear ethers (**2.24**–**2.26**), vinyl bromide (**2.23**), and toluene (**2.27**) with aryl bromides of different electronic nature. Aryl bromides bearing electron-withdrawing or electron-donating groups underwent this transformation with good to excellent yields. Notably, ester (**2.9**, **2.17**), ketone (**2.11**), amide (**2.12**), phenol and benzyl alcohol (**2.14** and **2.13**), aniline (**2.15**), boronate (**2.16**), alkene (**2.17**), and aldehyde (**2.18**) functionalities were perfectly tolerated in this reaction. An aryl chloride was also successfully employed, leaving the chloride moiety intact upon reaction completion (**2.10**), which provided an opportunity for further functionalization of the product. Electron-poor (pyridines) and electron-rich (thiophene) heterocycles did not interfere with the developed reaction protocol, furnishing products **2.19**–**2.22** in good yields.

Inspired by the broadness and success of the arylation reaction, the authors succeeded in expanding this protocol to alkylation reactions. This was achieved by switching the

Biographical Sketches

Valeriia Iziumchenko received her B.Sc. from the Moscow State University in Russia. In 2018, she joined the Gevorgyan group at the University of Illinois at Chicago as a Ph.D. student and later moved to the University of Texas at Dallas. Her research work is focused on the development of novel photoinduced methodologies.

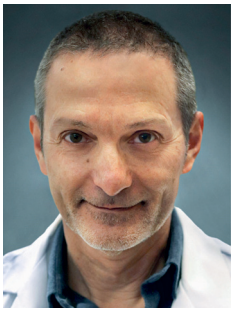

Vladimir Gevorgyan received his Ph.D. from the Latvian Institute of Organic Synthesis. After two years of postdoctoral research (1992–1994, JSPS and Ciba Geigy International Postdoctoral Fellowships) at Tohoku University, Japan, and a visiting professorship (1995) at CNR, Bologna, Italy, he joined the faculty at Tohoku University (Assistant Professor, 1996; Associate Professor, 1997–1999). In 1999, he moved to the United States to join the University of Illinois at Chicago (Associate Professor, 1999; Professor, 2003; LAS Distinguished Professor, 2012). In 2019, he joined The University of Texas at Dallas to become the Robert A. Welch Distinguished Chair in Chemistry. Vladimir also holds a professor position at the University of Texas Southwestern Medical Center. His group is interested in the development of novel synthetic methodology, particularly toward biologically relevant molecules.

ligand to 4,4′-di-*tert*-butyl-2,2′-bipyridine (**2.5**) and adding 1 equivalent of CF_3CO_2Na. Unactivated alkyl bromides possessing alkene (**2.28**), free alcohol (**2.29**), silyl ether (**2.30**), and aldehyde (**2.31**) moieties were accommodated under these conditions. It is worth mentioning that this method allowed for the formation of C(sp^3)–C(sp^3) bonds in several challenging substrates possessing particularly strong C(sp^3)–H bonds (**2.34**–**2.36**).

The proposed reaction pathway starts with the excitation of photocatalyst **2.3** to form triplet ketone biradical **A**. The latter abstracts hydrogen from substrate **2.1**, yielding alkyl radical **C** and ketyl radical **B**. At the same time, low-valent $L_nNi(0)$ **D** undergoes oxidative addition with the aryl or alkyl bromide (*Path a*), forming Ni(II) intermediate **E**, which subsequently recombines with the radical **C**. The obtained Ni(III) intermediate **F** undergoes reductive elimination, affording product **2.6** and Ni(I) species **G**, which undergoes single electron transfer with ketyl radical **B** ($E_{1/2}^{red}$ (**2.3**) = –2.05 V vs $Ag/AgNO_3$ in MeCN,[9a] E^{red} [Ni(I)/Ni(0)] ≈ –1.13 V vs $Ag/AgNO_3$ in DMF)[17] to recover the photocatalyst **2.3** and active Ni(0) catalyst **D**. Alternative *Path b* implies interception of the radical **C** by Ni(0), followed by oxidative addition of the organic halide to form Ni(III) complex **F**.

In this work, another mechanistic hypothesis was also considered. Under this scenario, HAT from the substrate molecule is accomplished by the bromine radical formed upon SET or EnT between Ni(II) entity **E** and the triplet ketone **A**.[18] However, this path was ruled out based on the following results. Firstly, the authors observed successful C–H arylation of cyclohexane using an aryl bromide (**2.37**). This reaction is unlikely to proceed via a bromine radical given the much weaker bond dissociation energy (BDE) in H–Br (87.5 kcal/mol) vs the strength of the C–H bond in cyclohexane (BDE = 98.6 kcal/mol).[19] Moreover, the formation of products **2.9** and **2.37** from aryl iodides further strengthens the argument against the involvement of halogen radicals, as in these cases the formed H–I bond (71.3 kcal/mol) would be significantly weaker than the C–H bonds in the substrates.

In 2019, Rueping's group reported C–H arylation in benzylic systems using synergistic catalysis with 4,4′-dichlorobenzophenone (**3.3**) and $NiCl_2{\cdot}6H_2O$/dtbbpy (Scheme 3).[20]

Aryl bromides with electron-deficient substituents at the *para* position underwent this reaction smoothly, providing products **3.5**–**3.7** in good yields. In the case of 1-bromo-4-chlorobenzene, bromine selectively reacted over chlorine, yielding product **3.7** in a good yield. Electron-rich aryl bromides also proved to be good coupling partners. Notably, an increase of steric hindrance caused by the introduction of *ortho* substitution did not diminish the efficiency (**3.11**). It should be mentioned, that bromotoluene substrates never performed as H-donors, which is likely due to a much higher concentration of toluene compared to the

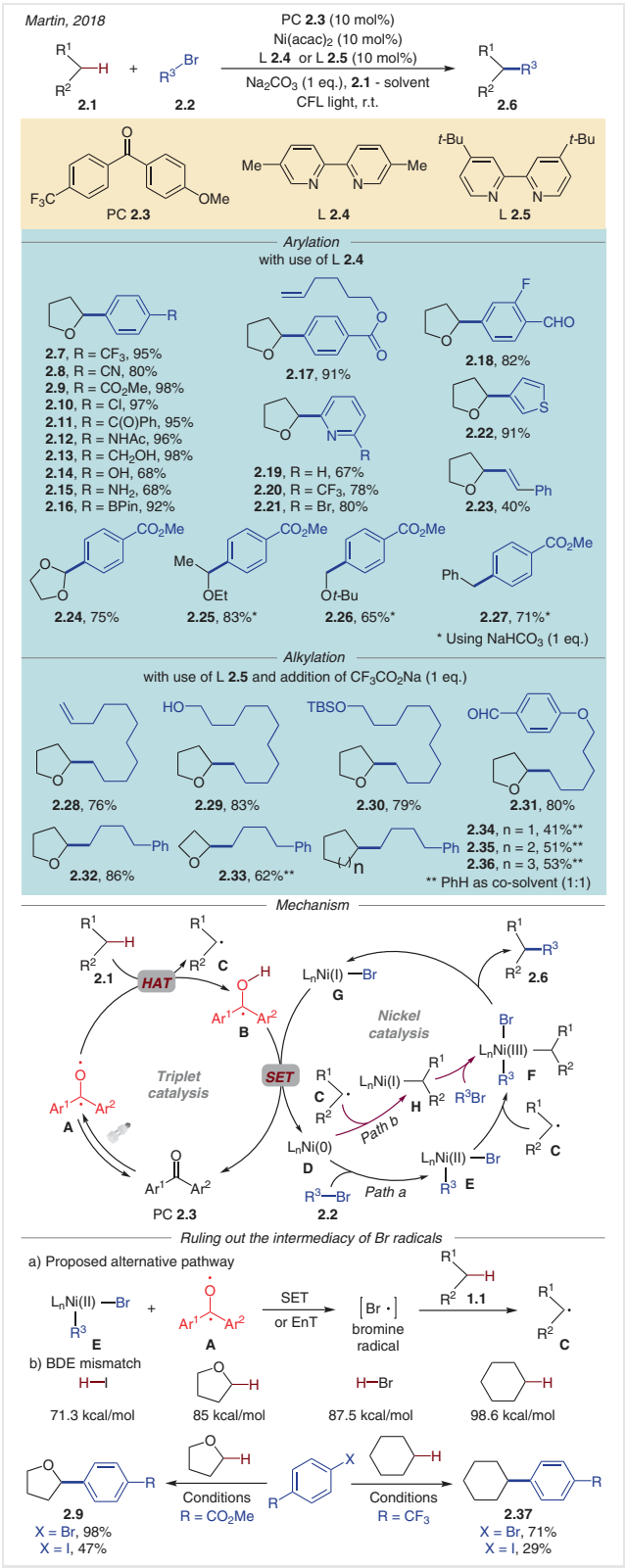

Scheme 2 C(sp^3)–H arylation and alkylation

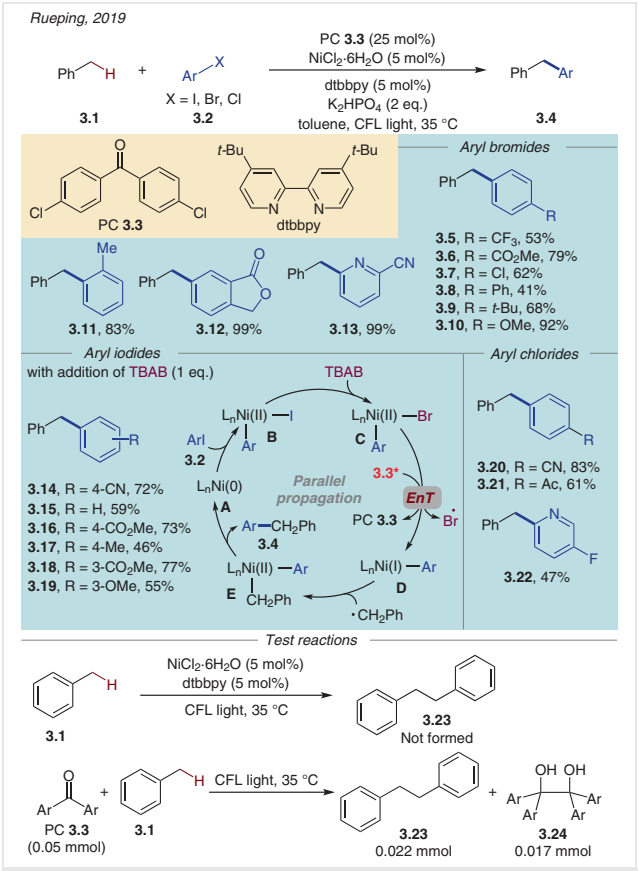

Scheme 3 Benzylic C–H arylation

aryl bromide. Substrates with fused rings and heterocyclic aryl bromides were highly efficient in this reaction (**3.12**, **3.13**).

The authors encountered decreased reactivity with aryl iodides compared to that of aryl bromides. This obstacle was solved by the addition of 1 equivalent of tetrabutylammonium bromide (TBAB) to the reaction mixture. The beneficial role of TBAB was explained in the proposed parallel propagation mechanism. According to this path, triplet ketone **3.3*** performs energy transfer to Ni(II) intermediate **C**, which is formed via halide exchange between **B** and TBAB, resulting in its homolysis to yield Ni(I) entity **D** and a bromine radical. The latter can potentially be engaged in HAT from benzylic substrates with weak C–H bonds.

Notably, aryl chlorides proved efficient coupling partners, furnishing products **3.20**–**3.22** in moderate to good yields.

Aside from the parallel propagation pathway described above, the reaction follows the same mechanism as that proposed by Martin (see Scheme 2).[16] This conclusion was verified by additional test reactions. Thus, bibenzyl **3.23**, originated from homocoupling of benzyl radicals, was a side product in arylation reactions. The formation of bibenzyl from toluene was not observed in the presence of the $NiCl_2$/dtbbpy combination under light. This disproves potential evolvement of a chlorine radical in the HAT step, resulting from homolysis of a light-excited $NiCl_2$ complex. However, bibenzyl was formed in presence of **3.3**. In addition, another common side product in triplet-ketone-mediated HAT transformations, benzopinacol **3.24**, was formed via recombination of ketyl radicals. This undesired reactivity of ketyl radicals often necessitates higher loadings of the ketone catalyst.[21] The observations discussed above confirm that triplet ketone acts as an initiator and a photocatalyst in this transformation. Overall, 4,4′-dichlorobenzophenone is considered to operate via both HAT and EnT pathways in benzylic C(sp^3)–H arylation.

Next, the same group developed a methodology for the synthesis of unsymmetrical ketones via direct benzylic acylation (Scheme 4).[22] In this transformation ketone **4.3** was used. This photocatalyst does not bear any halogen atoms, which eliminates the possibility of nickel-catalyzed side reactions.

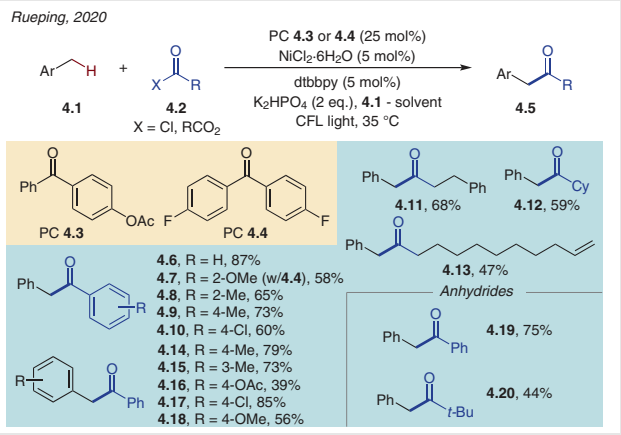

Scheme 4 Synthesis of unsymmetrical ketones via direct benzylic acylation

First, a range of benzoyl chlorides was subjected to the reaction with toluene. A methyl group was tolerated at both *para* and *ortho* positions giving 73% and 65% yields of the corresponding products (**4.9**, **4.8**), respectively. To engage substrates with more polar groups, ketone **4.3** was replaced with **4.4**, which helped with the product separation (**4.7**). Aliphatic acyl chlorides, hydrocinnamoyl chloride and cyclohexanecarboxylic acid chloride also delivered ketones in moderate yields (**4.11**, **4.12**). A long-chain acid chloride bearing a terminal alkene was suitable for this transformation (**4.13**). Anhydrides were also capable substrates in this reaction (**4.19**, **4.20**). Finally, the employment of substituted toluene derivatives with benzoyl chloride posed no problems in this reaction, furnishing products **4.14**–**4.18** in good yields.

Another transformation following the same mechanism was developed by Luo's group in 2021 (Scheme 5).[23] They demonstrated the acylation of toluene and its derivatives

with *N*-acylsuccinimides. The catalytic system consisting of 4,4′-dichlorobenzophenone photocatalyst **5.3** and $NiCl_2$·DCE/dtbbpy operates under UVA irradiation.

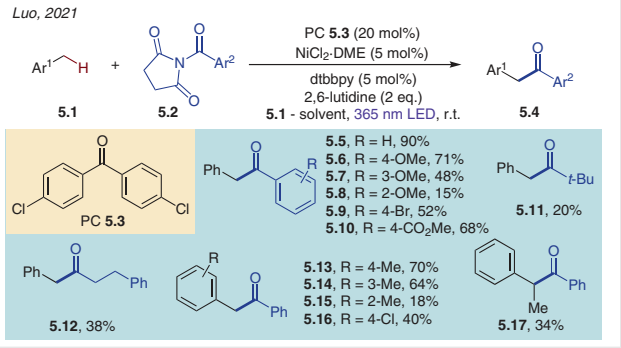

Scheme 5 Activation of C(sp^3)–H bonds in acylation reactions

A study of the reaction scope indicated less influence of the electronic factors, as it proceeded well with aromatic substrates possessing both electron-donating (**5.6**–**5.8**) and electron-withdrawing (**5.9**, **5.10**) groups. However, sterically more hindered amides were less efficient (**5.7**, **5.8**). Aliphatic *N*-acylsuccinimides also underwent coupling with toluene, albeit providing products in diminished yields (**5.11**, **5.12**). The reaction efficiency was also affected by the sterics of toluene derivatives (**5.13**–**5.15**). Notably, ethylbenzene was efficiently activated by ketone **5.3**, furnishing product **5.17** in moderate yield.

In 2019, König disclosed a mechanistically interesting transformation, where a light-absorbing ketone is formed and then serves as a photocatalyst. In this protocol, benzaldehyde derivatives were coupled with aryl bromides in acetone under Ni(dmbpy)Br_2 (dmbpy = 4,4′-dimethyl-2,2′-bipyridyl) catalysis and 395 nm light irradiation (Scheme 6).[24]

Aryl bromides substituted with electron-withdrawing groups, such as cyano, ester, triflate, or halogens, underwent efficient coupling with 4-chlorobenzaldehyde, affording products **6.4**–**6.8** in good yields. Heterocyclic bromides furnished unsymmetrical ketones **6.9** and **6.10** in moderate yields. Both electron-rich and electron-deficient benzaldehydes were efficient substrates in this transformation, leading to products **6.11**–**6.15** in good to excellent yields.

Species responsible for the reaction initiation are believed to be a reacting aldehyde along with benzil and benzophenone, formed upon benzaldehyde photolysis, homocoupling, and a subsequent decarboxylation. The excited carbonyl biradical **E** abstracts hydrogen from the aldehyde, delivering acyl radical **F** and ketyl radical **G**. The Ni(0) catalyst is transformed into complex **B** upon oxidative addition with **6.2**. The latter traps acyl radical **F** to form Ni(III) intermediate **C**, which upon reductive elimination provides diaryl ketone **6.3** and Ni(I) species **D**. Reaction product **6.3** now

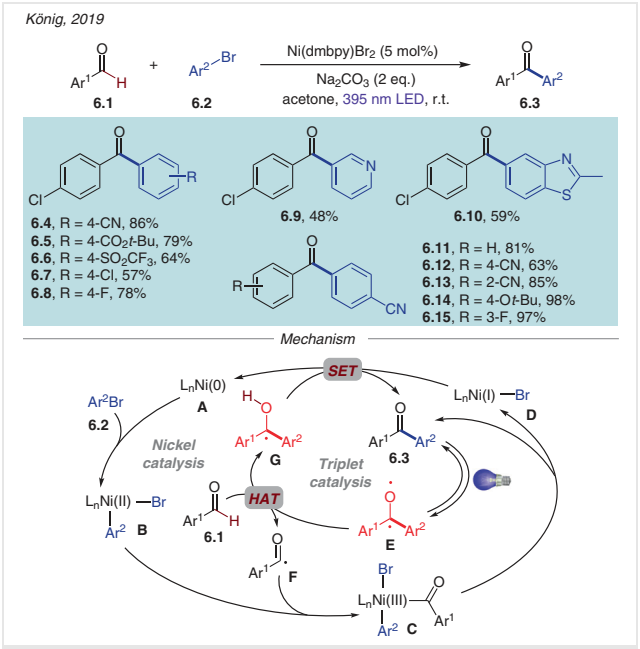

Scheme 6 Benzoylation of aryl bromides

becomes a photocatalyst for further catalytic cycles. Ketyl radical **G** recovers to **6.3** through SET with **D**, which also results in Ni(0) complex recovery.

In the same year, Murakami and co-workers discovered the photocatalytic carboxylation of benzylic and aliphatic bonds with carbon dioxide (Scheme 7).[25] This transformation represents the first example of direct CO_2 fixation with benzylic substrates and saturated hydrocarbons via homogeneous catalysis.

The catalytic system for benzylic carboxylation includes xanthone **7.3**, $NiCl_2$·$6H_2O$/$(2\text{-Py})_2CH_2$ (di(2-pyridyl)methane) and *t*-BuOK in benzene. Using this method, *p*-xylene and *p*-methoxytoluene were smoothly carboxylated, providing products **7.9** and **7.8** in good yields. Notably, no dicarboxylation occurred at the second benzylic moiety of xylene, probably due to the reduced solubility of the forming carboxylate salt in benzene. 4-Fluoro-, 4-chloro-, and 4-methoxy-3-cyanotoluene were transformed into the corresponding carboxylic acids (**7.6**, **7.7**, **7.10**), albeit with diminished yields. These electron-deficient substrates are somewhat electron-mismatched with the electrophilic oxygen-centered radical of triplet ketone, which prefers HAT from electron-rich C–H bonds. Importantly, the authors succeeded in the carboxylation of simple aliphatic hydrocarbons. For this reaction, 4,4′-di-*tert*-butylbenzophenone (**7.12**) as the photocatalyst and 4,4′-dimethoxy-2,2′-bipyridine ligand (**7.13**) were used. Under atmospheric CO_2 pressure, cyclohexane was transformed into cyclohexanecarboxylic acid **7.14** in 80% yield, based on the amount of *t*-BuOK used.

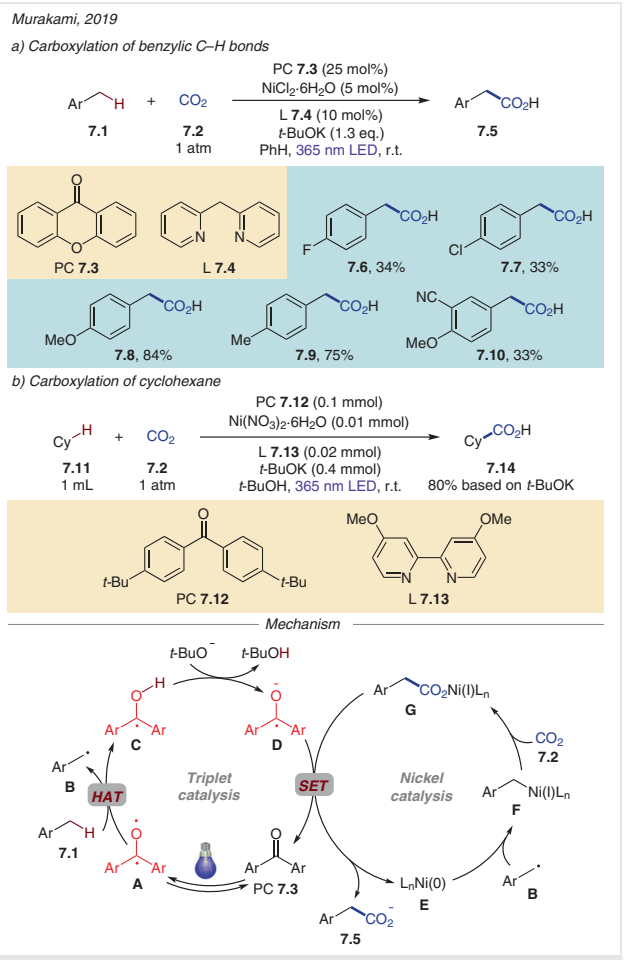

Scheme 7 Carboxylation of benzylic and aliphatic C–H bonds with CO_2

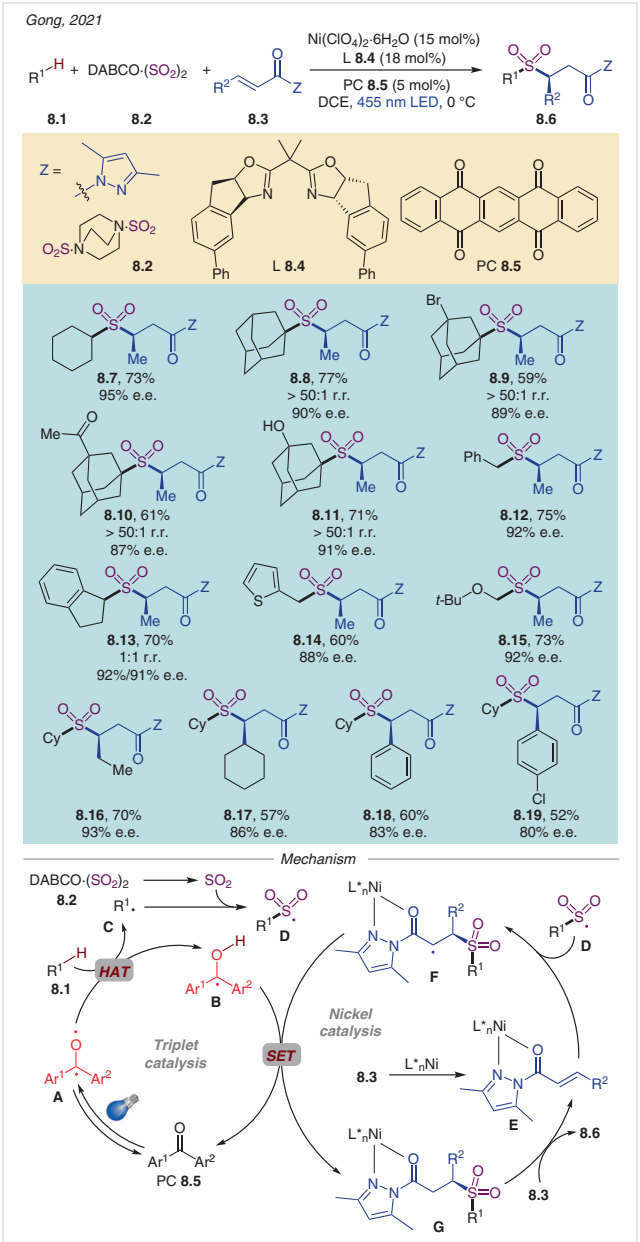

Scheme 8 Three-component asymmetric sulfonylation

The mechanism of this transformation begins with benzylic hydrogen abstraction by triplet ketone **A**. The formed ketyl radical **C** is deprotonated by *tert*-butoxide to yield radical anion **D**. Meanwhile, benzylic radical **B**, formed upon HAT, recombines with $L_nNi(0)$, generating benzylnickel(I) intermediate **F**. Carbon dioxide inserts into the C–Ni(I) bond of **F** leading to Ni(I) carboxylate **G**, which is reduced by ketyl radical anion **D** to Ni(0). This SET process releases the resulting carboxylate anion **7.5** and recovers photocatalyst **7.3**.

In 2021, Gong's group developed a three-component asymmetric sulfonylation reaction (Scheme 8).[26] Coupling of α,β-unsaturated carbonyls, bearing an *N*-acylpyrazole moiety, with SO_2 and H-donors occurred in enantioselective fashion with employment of $Ni(ClO_4)_2·6H_2O$ as the catalyst, chiral ligand **8.4**, and 5,7,12,14-pentacenetetrone (**8.5**) under visible light at 0 °C. The authors chose DABCO·$(SO_2)_2$ as a SO_2 surrogate.

Cycloalkanes of different ring sizes underwent the reaction efficiently, delivering products in high yields and enantioselectivity (**8.7**). Challenging tertiary adamantane C–Hs (BDE = 99 kcal/mol) regioselectively underwent sulfonylation (**8.8**–**8.11**). Moreover, several functionalities, such as halogen, ketone, and free alcohol, were perfectly tolerated giving rise to the corresponding chiral sulfones with 87–91% e.e. The employment of primary and secondary benzylic substrates resulted in the formation of products **8.12** and **8.13** in good yields. Heteroaromatic H-donor 2-methylthiophene was compatible with the reaction protocol furnishing product **8.14** with 88% e.e. Ethers were also suitable

substrates in this reaction (**8.15**). Lastly, the authors tested α,β-unsaturated *N*-acylpyrazoles. Linear, cyclic, and aryl β-substituents posed no problems for this transformation, providing chiral sulfones **8.16**–**8.19** in yields of 52–70% and with satisfactory e.e. values.

A plausible mechanism for this reaction starts with excitation of photocatalyst **8.5** and subsequent HAT from H-donor **8.1** to the ketone biradical **A**. The formed transient carbon radical **C** is trapped by sulfur dioxide, released *in situ* from DABCO·$(SO_2)_2$, to generate sulfonyl radical **D**. Simultaneously, the chiral L^*_nNi catalyst undergoes ligand exchange with α,β-unsaturated *N*-acylpyrazole **8.3**, yielding species **E**, which intercepts sulfonyl radical **D**. The resulting radical complex **F** engages in SET and proton transfer with ketyl radical **B** and a small amount of water, recovering ketone **8.5** and affording neutral complex **G**. The latter goes through ligand exchange with substrate **8.3**, releasing the product of the transformation and substrate-coordinated chiral complex **E**.

Molander, in 2021, demonstrated another three-component coupling protocol, where activated olefins were dicarbofunctionalized with aryl halides and C(sp^3)–H-possessing substrates (Scheme 9).[27] In this method, push–pull diaryl ketone **9.4** was utilized as a photocatalyst in tandem with Ni(dtbbpy)Br_2 under 390 nm LED irradiation.

A number of aryl and heteroaryl bromides were employed in the reaction with cyclopentyl methyl ether as a H-donor and *tert*-butyl acrylate. Aryl bromides bearing electron-withdrawing groups showed the best reactivity, providing products in good yields (**9.7**, **9.8**). Substrates with functional handles, like Bpin or halogens, afforded products of dicarbofunctionalization in moderate yields, raising the opportunity for further diversification of these molecules (**9.10**, **9.11**). Heteroaryl bromides were also compatible with the reaction conditions (**9.13**, **9.14**). Thus, flumazenil, an arene derived from a GABA-receptor antagonist, delivered dicarbofunctionalized product **9.12** in moderate yield with the use of *i*-PrOH as the C–H component. Ethers and thioethers were also capable substrates (**9.14**, **9.15**). α-Amido C–H bonds could also be successfully employed leading to a single α-amido-functionalized regioisomer **9.17**. Importantly, the authors demonstrated the first case of photocatalyzed HAT from an α-boronate C–H bond, achieving the synthesis of routinely functionalizable boronate **9.18** in moderate yield. Notably, not only terminal, but also internal alkenes participated in this transformation, delivering products in good yields and diastereoselectivity (**9.19**, **9.20**).

The proposed mechanism begins with the excitation of photocatalyst **9.4** and its conversion into the triplet state **A**. It then forms alkyl radical **B** and ketyl radical **C** via HAT from **9.1**. Notably, push–pull ketones bearing electron-rich and electron-deficient aromatic rings were most efficient in the HAT step and provided the best yields. This can be linked to the longer triplet lifetimes of these molecules, attributed to the captodative radical stabilization.[28] Alkyl radical **B** then undergoes Giese-type addition to activated alkene **9.2** yielding radical species **D**. On the other hand, aryl halide **9.3**, via oxidative addition to $L_nNi(0)$, furnishes Ni(II) complex **F**, which in turn intercepts radical **D** to form Ni(III) adduct **G**. The latter, upon reductive elimination, releases the product **9.5** and delivers Ni(I) entity **H**, which via SET from ketyl radical **C** is reduced to Ni(0) and oxidizes **C** to **9.4**, thus completing both catalytic cycles. Noteworthy, according to density functional theory (DFT) calculations, an alternative mechanistic pathway involving interception of radical **D** by Ni(0), hence preceding the oxidative addition step with aryl bromide, is also feasible. Notably, a high concentration of alkene is essential for this protocol to avoid direct addition of radical **B** to nickel (which would result in a two-component cross-coupling product) and to promote irreversible Giese-type addition to the activated alkene.

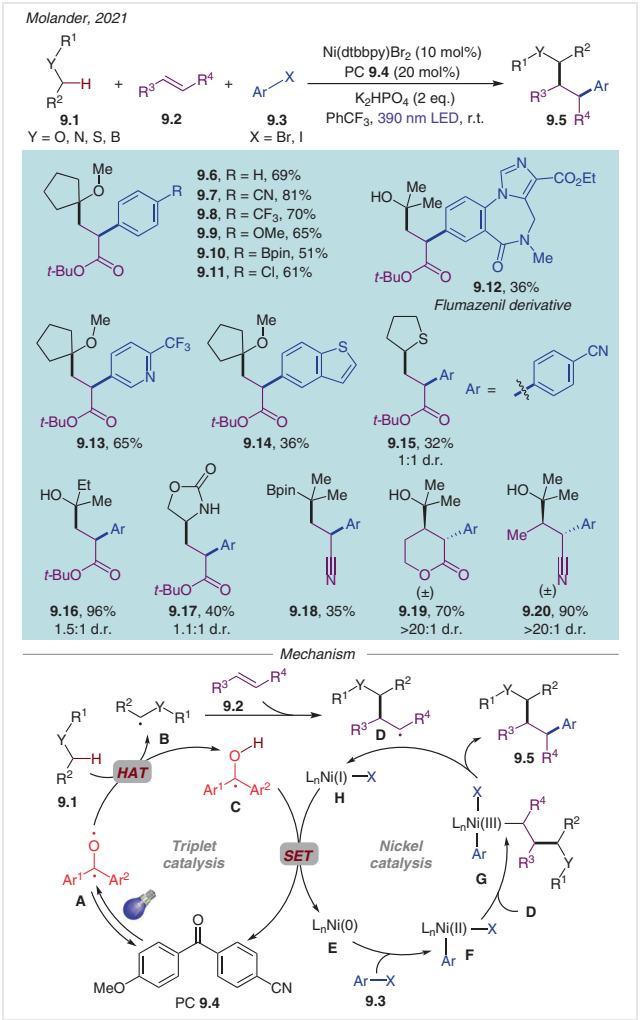

Scheme 9 Dicarbofunctionalization of olefins

An elegant method for cross-electrophile coupling and olefin dicarbofunctionalization, both in batch and flow, was disclosed by Noël in 2022.[29] This protocol features light-absorbing benzophenone as a HAT photocatalyst, superstoichiometric silane as a halogen atom transfer (XAT) agent, and Ni(dtbbpy)Br_2 as a transition-metal catalyst (Scheme 10).

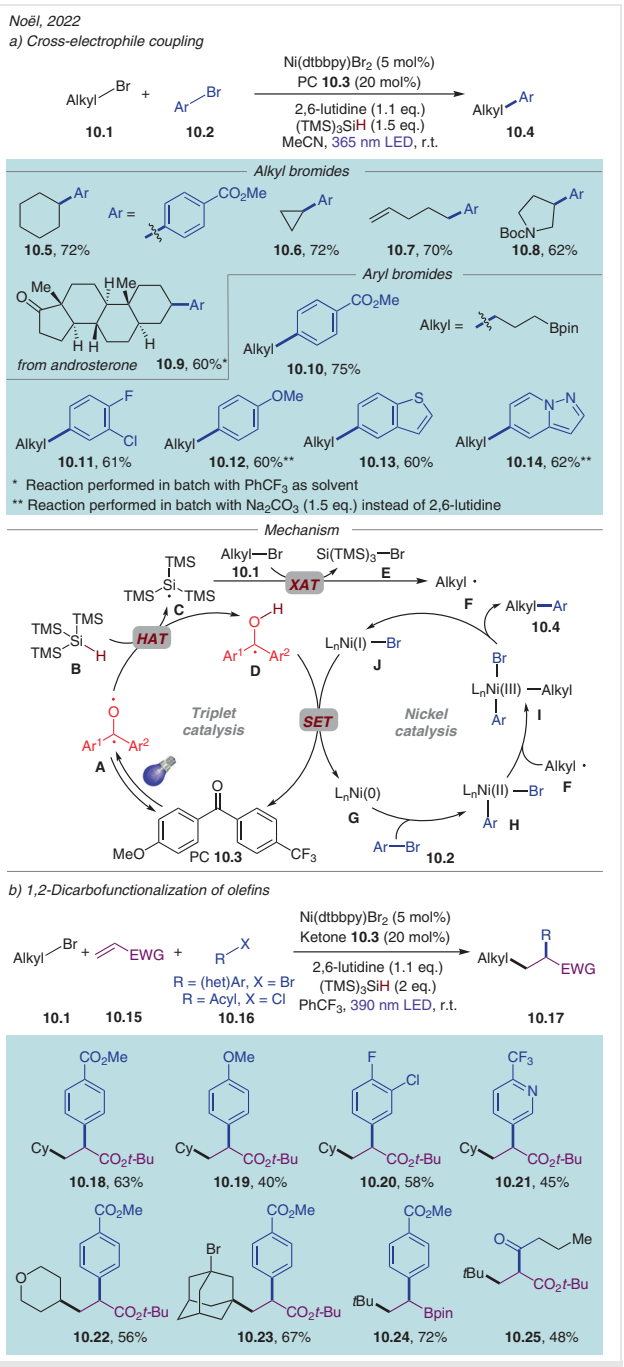

Scheme 10 Cross-electrophile coupling and 1,2-dicarbofunctionalization of olefins enabled by the merger of benzophenone HAT photocatalysis and silyl-radical-induced halogen atom transfer

Cross-electrophile coupling between alkyl bromides and aryl bromides was performed mostly under flow conditions. The authors found secondary cyclic and heterocyclic alkyl bromides to be suitable for this transformation regardless of the size of the ring (**10.5**, **10.6**, **10.8**). Notably, heterocyclic alkyl bromides containing oxygen or nitrogen atoms delivered no byproducts originating from a competing HAT from α-to-heteroatom C–H bonds. Primary alkyl bromides were excellent coupling partners as well (**10.7**). The applicability of the developed method under complex settings was demonstrated by the successful arylation of an androsterone derivative (**10.9**). Both electron-poor and electron-rich aryl bromides were efficient in this transformation (**10.10**, **10.12**). A polyhalogenated arene selectively furnished the coupling product at the bromine site (**10.11**), opening the prospect for further aryl ring functionalization. Heteroaryl bromides were also efficiently alkylated, forming the corresponding products in good yields (**10.13**, **10.14**).

1,2-Dicarbofunctionalization of olefins was performed under slightly altered conditions. The scope of this reaction included electron-rich and electron-deficient aryl bromides along with difunctionalized and heterocyclic derivatives (**10.18**–**10.21**). Dibromo adamantane underwent monofunctionalization with one bromide moiety remaining untouched (**10.23**). Notably, vinyl pinacol borane also reacted well, providing a handle for further diversification (**10.24**). In addition, an acyl chloride could be used in place of the aryl bromide to form 2-substituted 1,3-dicarbonyl compound (**10.25**).

Mechanistically, these transformations closely resemble those previously described. The difference is that here ketone biradical **A** abstracts hydrogen from supersilane **B**. The generated silyl radical **C** is very halophilic, so it is capable of bromine abstraction from alkyl bromide **10.1**. The produced alkyl radical **F** then enters the nickel catalytic cycle, adding to Ni(II) species **H**, formed from Ni(0) upon oxidative addition with the aryl bromide. The resulting adduct **I** undergoes reductive elimination, delivering the product **10.4** and Ni(I) species **J**. The latter engages in SET with ketyl radical **D**, thus leading to recovery of the catalysts.

2.2 Triplet Ketones with Copper Catalysis

In 2016, Murakami demonstrated carboxylation of allylic C–H bonds of alkenes with carbon dioxide using 3,6-diphenyl-9*H*-xanthone (**11.4**) and copper carbene complex **11.3** under UVA light irradiation at elevated temperature (Scheme 11).[30]

For the carboxylation of cyclohexene (**11.6**), a turnover number (TON) for the copper catalyst was found to be 45, and was slightly higher for the carboxylation of cyclopentene (**11.7**). Tetrasubstituted olefin **11.8** was carboxylated at the most sterically hindered position (**11.9**), whereas un-

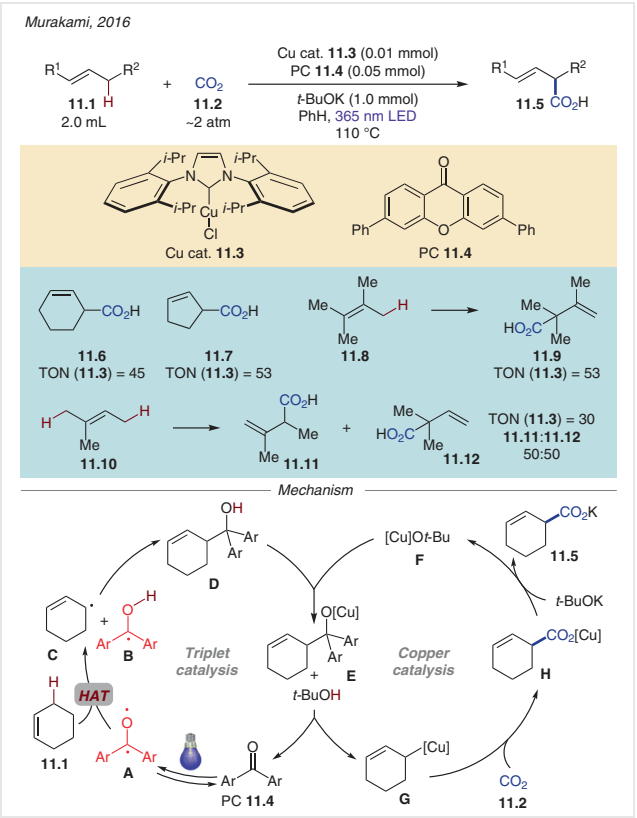

Scheme 11 Carboxylation of allylic C–H bonds of alkenes with CO_2

symmetrical trisubstituted alkene **11.10**, possessing two distinct allylic C–Hs, reacted in an unselective manner (**11.11**, **11.12**).

The proposed mechanism commences with the UV light excitation of xanthone **11.4** and intermolecular HAT of the allylic hydrogen atom by the oxygen-centered radical of **A**. This event results in formation of radical pair **C** and **B**, which upon recombination gives rise to homoallylic alcohol **D**. The latter is deprotonated by copper *tert*-butoxide (**F**) to generate copper alkoxide **E**, which upon β-carbon elimination liberates the photocatalyst and generates allylcopper species **G**. A subsequent nucleophilic addition of **G** to CO_2 results in the formation of copper carboxylate **H**. A subsequent ligand exchange with *t*-BuOK then delivers the product **11.5** and regenerates [Cu]O*t*-Bu.

In 2019, Vincent disclosed the Giese-type alkylation of alkenes by radicals generated via HAT from C(sp^3)–H sites of substrates driven by tandem copper/benzophenone (**BP**) photocatalysis (Scheme 12).[31]

Boc-protected cyclic amines reacted well with activated olefins, delivering products **12.4**–**12.6** in moderate yields. Notably, *N*,*N*-dimethylbenzylamine gave the product of selective HAT at the C(sp^3)–H site of the methyl group with the benzylic C(sp^3)–H moiety remaining intact (**12.8**). Alpha-to-oxygen C(sp^3)–H bonds were activated via this method, affording products **12.7**, **12.9**, and **12.10** in good

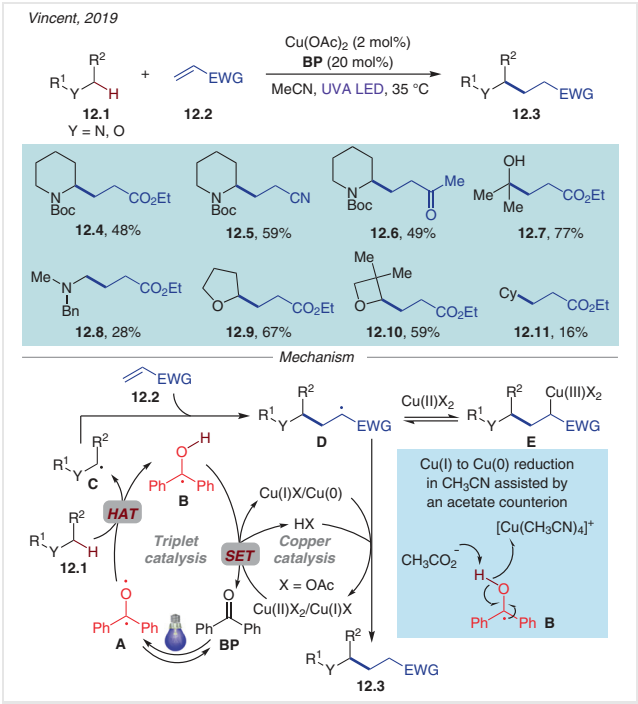

Scheme 12 Giese-type alkylation of C(sp^3)–H bonds

yields from isopropanol, THF, and 3,3-dimethyloxetane, respectively. Moreover, alkylation with cyclohexane was achieved in 16% yield (**12.11**).

Mechanistic studies, carried out by the authors, suggested the following reaction pathway. UV-light-generated triplet benzophenone **A** performs HAT from substrate **12.11**, thus leading to radical species C that adds to the Michael acceptor **12.2** to give **D**. The latter at earlier stages of the reaction can be intercepted by copper acetate to form metastable Cu(III) complex **E**, which is considered to be a masked radical that helps to prevent undesired radical-initiated polymerization of the alkene. Simultaneously, ketyl radical **B** reduces Cu(I) to Cu(0) (or Cu(II) to Cu(I)), returning **BP** to the catalytic cycle. The formed Cu(0) (or Cu(I)) transfers an electron to alkyl radical species **D**, which, after a subsequent protonation, delivers the reaction product **12.3**. Interestingly, the use of other copper salts as catalysts resulted in alkene polymerization. This might be attributed to the crucial role of the acetate counterion serving as a base in a proton-coupled electron transfer from ketyl radical **B**, leading to the essential Cu(I) to Cu(0) reduction.

In the same year, Gong's group published their work on stereoselective C(sp^3)–H functionalization of benzylic/allylic hydrocarbons and unactivated alkanes (Scheme 13).[32] In this protocol, the combination of a copper or a cobalt tetrafluoroborate catalyst, a chiral bisoxazoline (BOX) ligand (**13.4** or **13.5**), and 5,7,12,14-pentacenetetrone under blue LED irradiation allowed the reaction between H-donors and *N*-sulfonylimines to proceed in a regio- and stereoselective fashion.

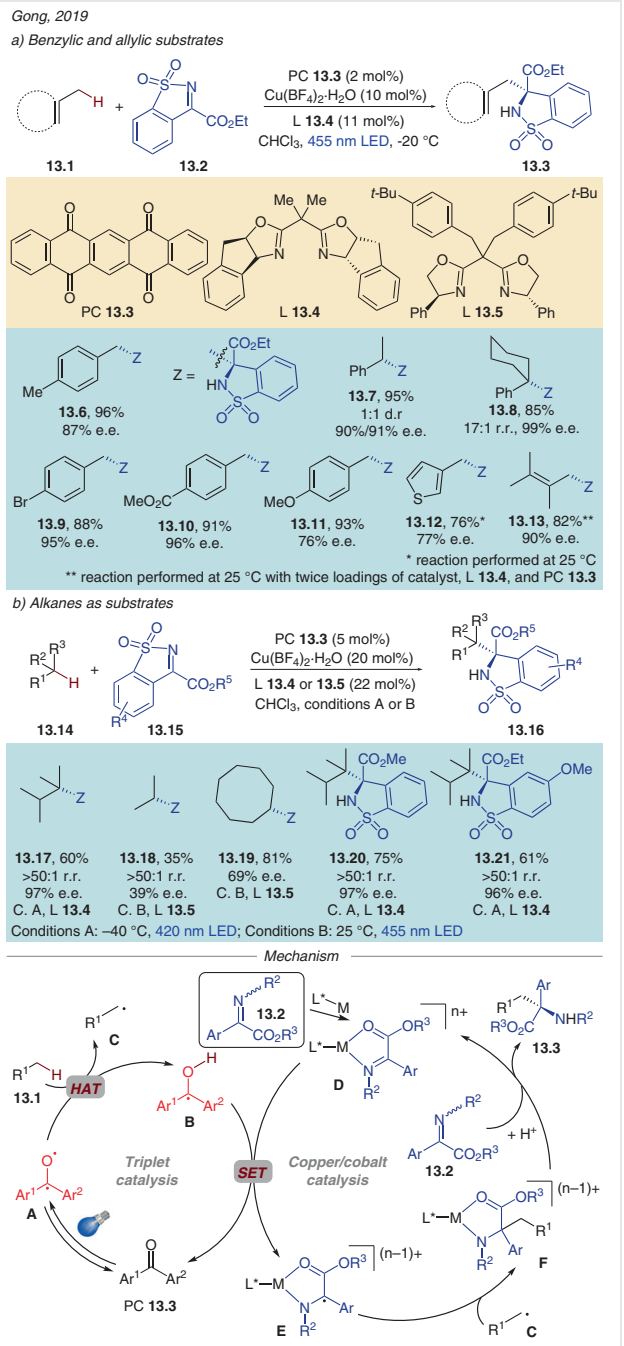

Scheme 13 Regio- and stereoselective C(sp^3)–H functionalization of benzylic/allylic hydrocarbons and unactivated alkanes

Thus, primary, secondary, and tertiary benzylic substrates provided products in excellent yields (**13.6–13.8**) and high enantioselectivity. A study of the functional group tolerance indicated that this method was quite general. Hence, toluene derivatives containing electron-withdrawing or electron-donating functionalities, as well as 3-methylthiophene, were compatible with the reaction conditions, affording the products **13.9–13.12** in high yields and enantioselectivity. Among allylic hydrocarbons subjected to the system, 2,3-dimethyl-2-butene delivered the product **13.13** in 82% chemical yield and with 90% e.e. Next, the authors successfully applied this photocatalytic system to the functionalization of stronger C–H bonds of simple alkanes. 2,3-Dimethylbutane furnished the product **13.17** in good yield and excellent e.e. Remarkably, very small molecules (like propane) could also be employed in this transformation, albeit delivering products in modest yield and with diminished enantioselectivity (**13.18**). Secondary C–H bonds of cycloalkanes also proved suitable for this transformation, delivering products with higher e.e. values for substrates with larger ring sizes (**13.19**). Imine substrates with different α-carbonyl groups, as well as those bearing electron-poor or electron-rich substituents at the phenyl-sulfonyl ring, underwent this reaction smoothly, delivering products **13.20** and **13.21** with over 95% e.e.

A plausible mechanism for this reaction starts with light-generated triplet ketone **A** performing HAT from **13.1**, affording transient alkyl radical **C** and ketyl radical **B**. At the same time, the chiral metal catalyst coordinates to the imine substrate **13.2**, leading to complex **D**. The latter is reduced via SET with ketyl radical **B**, which yields recovered ketone **13.3** and persistent radical **E**. This radical species couples with radical **C**, affording complex **F** with stereoselectivity defined by the chiral ligand–metal scaffold. A subsequent protonation and ligand exchange with the new portion of the imine furnishes the product and regenerates complex **D**.

The same group recently disclosed site-selective sulfonylation of benzylic C–H bonds in the presence of sodium sulfinates, stoichiometric copper(II) triflate, and catalytic 5,7,12,14-pentacenetetrone under 410 nm light irradiation (Scheme 14).[33]

Ethylbenzene derivatives bearing electron-donating groups at the *para* position of the phenyl ring all delivered products in good yields (**14.5–14.8**). Secondary benzylic substrates with a longer alkyl chain decorated with distinct functionalities also performed well in this reaction (**14.9**, **14.10**). Examples of sulfonylated tertiary benzylic substrates were less efficient. Altering the sodium sulfinates allowed the authors to employ substrates with different aryl or heteroaryl substituents (**14.11–14.13**), as well as an example bearing a trifluoromethyl group on the sulfone moiety (**14.14**). Within unactivated H-donors, cycloalkanes were capable partners for this protocol, providing products (**14.15**), albeit in lower yield than their benzylic counterparts. Celestolide was also regioselectively functionalized (**14.16**).

The proposed mechanism for this sulfonylation reaction commences with HAT from substrate **14.1**. by ketone biradical **A** to generate carbon-centered radical **C** and ketyl radical **B**. Meanwhile, copper(II) triflate reacts with sodium sulfonate, resulting in the formation of complex **D**, which traps radical **C** to yield Cu(III) intermediate **E**, that upon reductive

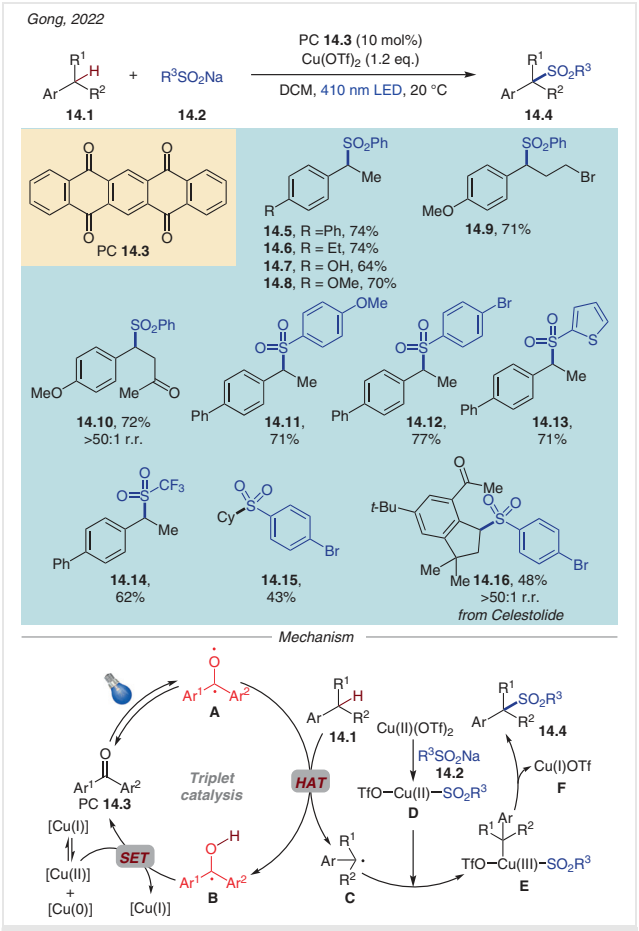

Scheme 14 Site-selective C(sp^3)–H sulfonylation of toluene derivatives and cycloalkanes with inorganic sulfinates

elimination liberates the sulfonylation product **14.4** and copper(I) triflate **F**. Disproportionation of the latter results in the formation of Cu(II) and Cu(0) species. Subsequently, the Cu(II) entity undergoes SET with ketyl radical **B** to recover the ketone.

In 2022, Liu demonstrated highly efficient and enantioselective benzylic C–H cyanation enabled by a merger of electro-/photo-/copper catalysis (Scheme 15).[34] In this system, the authors altered the utilized photocatalyst based on the electronics of the substrate to match the HAT ability of the anthraquinone (**AQ^{R}**) with each H-donor.

As the process of photocatalysis is decoupled from the copper catalysis, the independent tuning of applied current allowed the control of Cu(II)/Cu(I) speciation, which is essential for the radical-trapping step. Overall, this decoupled radical relay protocol granted an appreciably expanded substrate scope and outstanding functional group tolerance in comparison with the existing coupled radical-relay method.[35]

Stern–Volmer quenching experiments with anthraquinones in the presence of benzylic substrates were included in the range of undertaken mechanistic studies. They re-

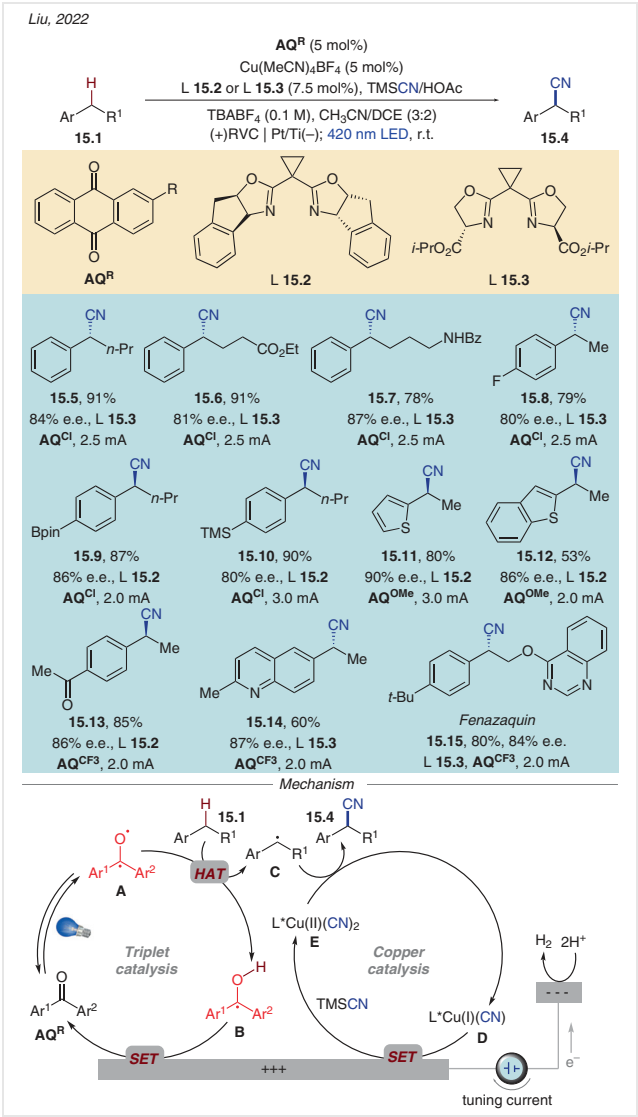

Scheme 15 Enantioselective benzylic C–H cyanation enabled by electrophotocatalytic decoupled radical relay

sulted in insightful conclusions helping to pick an **AQ^{R}** for different substrates. More electron-deficient anthraquinones (**AQ^{CF3}**) were more suitable for electron-poor benzyl substrates, whereas electron-richer photocatalysts (**AQ^{Me}**, **AQ^{OMe}**) worked better for electron-rich alkylarenes. These trends can be seen in the reaction scope.

Benzylic substrates possessing ester or amide functionalities on alkyl chains worked well in this reaction, delivering products **15.6** and **15.7** in excellent yields and with good enantioselectivity. Functionalities on the phenyl ring, including halogens or even oxidation-sensitive boronate and silane were tolerated in this protocol, affording enantio-enriched products **15.8**–**15.10** in good yields. Electron-rich substrates, containing thiophene and benzothiophene scaffolds, were also successfully employed in this transfor-

mation with the use of more electron-rich **AQ^{OMe}** (**15.11**, **15.12**). In contrast, alkylarene substrates bearing an electron-deficient ketone or quinoline required the use of electron-poor **AQ^{CF3}** to furnish nitriles **15.13** and **15.14**. It was also shown that the pesticide fenazaquin could be enantioselectively functionalized to give **15.15** in 80% yield and 84% e.e.

The proposed mechanism begins with photoexcitation of the **AQ^{R}** photocatalyst, followed by its conversion into the triplet excited state **A**, which abstracts a benzylic hydrogen from the alkylarene substrate **15.1** to generate benzylic radical **C** and ketyl radical **B**. The capture of radical **C** by L*Cu(II)(CN)$_2$ entity **E** subsequently yields nitrile product **15.4** and L*Cu(I)(CN) intermediate **D**. Both intermediate **D** and ketyl radical **B** are oxidized at the anode to recover Cu(II) species **E** and **AQ^{R}**, respectively. The authors claim that it is essential for better reactivity to match L*Cu(II)(CN)$_2$ generation with the rate of benzylic radical formation. This matching is achieved by tuning of the applied current.

2.3 Triplet Ketones with Other Transition-Metal Catalysis

There are only a few examples of the use of dual triplet ketone/transition-metal catalysis with metals other than nickel and copper.

In 2020, Zheng's group employed synergistic palladium/anthraquinone photocatalysis under visible light toward direct C–H arylation of aldehydes (Scheme 16).[36]

The scope of the aryl bromides used included electron-rich and electron-deficient substrates, as well as examples bearing chloride and a boronic ester. The latter two (**16.8**, **16.9**) are of a particular interest as they possess a handle for further diversification. Heteroaryl bromides can also be successfully employed (**16.10**). The reaction is quite general with respect to the aldehyde. Thus, linear primary aldehydes, cyclic and acyclic secondary aldehydes, alkyl aldehydes bearing double bonds, halides, and free alcohols can be employed. 4-Methoxybenzaldehyde was used under slightly modified reaction conditions, providing the product **16.11** in moderate yield.

The following reaction pathway was proposed based on DFT calculations. The excited anthraquinone **[AQ]***, generated upon irradiation of the photocatalyst with 427 nm light, engages in HAT with aldehyde **16.1** to give acyl radical **A** and and **AQ-H**, the reduced form of the ketone. Concomitantly, via *Path a*, Pd(0) undergoes oxidative addition with the aryl bromide to produce Pd(II) complex **C**, which upon acyl radical interception forms Pd(III) species **D**. Alternatively (*Path b*), the acyl radical can be coupled with Pd(0) first, followed by oxidative addition of the aryl bromide to complex **F** to reach the same intermediate **D**. The latter reductively eliminates the product **16.3** and regenerates Pd(I) entity **E**. The oxidation of **AQ-H** back to **AQ** is assisted by the base simultaneously with the reduction of Pd(I) to Pd(0).

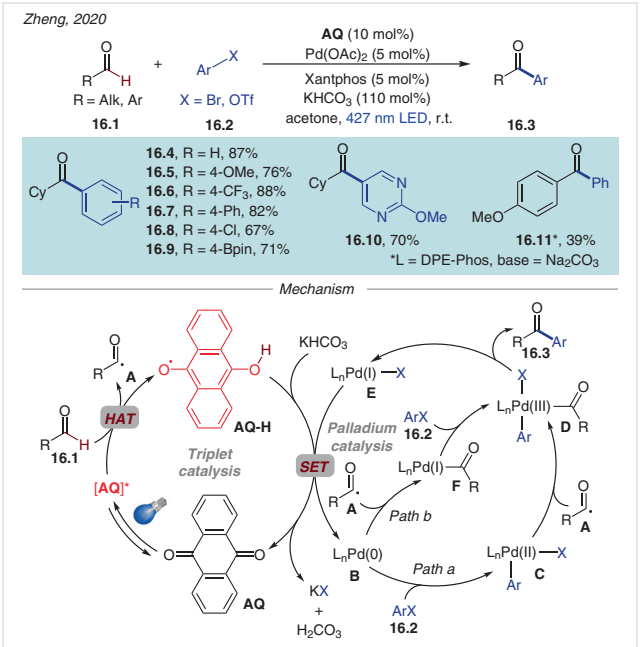

Scheme 16 Direct C–H arylation of aldehydes

In the same year, Lei reported an effective merger of metal catalysis, electrochemistry, and photochemistry in the oxidative azidation of C(sp^3)–H bonds (Scheme 17).[37] This protocol involved a manganese/1,10-phenanthroline catalyst, fluorenone (**17.3**), DDQ (**17.4**) or bis(4-methoxyphenyl)methanone (**17.5**) as the photocatalyst, and nucleophilic sodium azide as an azidation agent under electrophotocatalytic conditions.

Among benzylic substrates, triphenylmethane delivered the product of azidation **17.7** in almost quantitative yield, supposedly due to the enhanced stability of the trityl radical. Other tertiary benzylic substrates reacted smoothly, providing products in good to excellent yields. Notably, 1,4-diisopropylbenzene, bearing two identical tertiary C–H sites, gave the major product of monoazidation **17.10** (57%), accompanied by the minor product of diazidation (35%). Biologically and photochemically relevant alkylthioxanthone afforded product **17.11** in a moderate yield. Azidation of *o*-ethyltoluene resulted in the product of secondary benzylic C–H bond functionalization (**17.12**) in the presence of the unreactive primary benzylic C–H site. Alkylated benzothiophene proved to be a suitable substrate, yielding 32% of the product **17.13**. Substrates bearing a longer alkyl chain were also reactive in this protocol. Within unactivated substrates, cyclododecane reacted smoothly producing **17.17** in 31% yield. Remote tertiary C–H sites of long-chain benzoate esters underwent selective azidation under this protocol

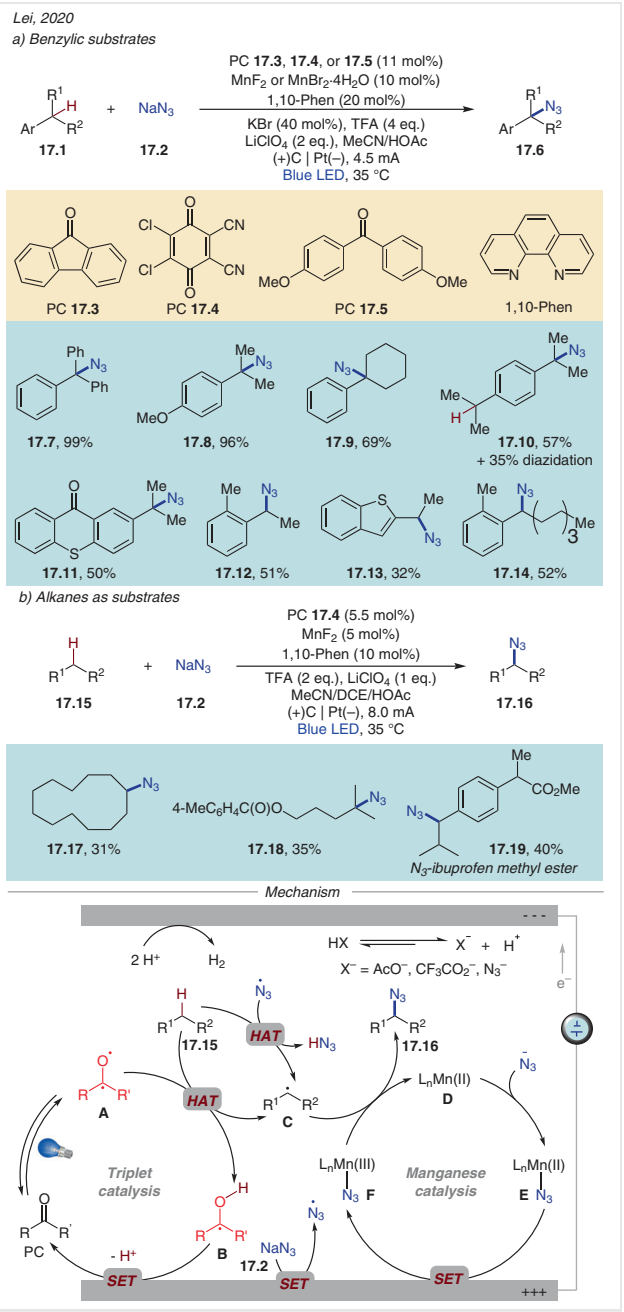

Scheme 17 Oxidative azidation of C(sp^3)–H bonds under electrophotocatalytic conditions

(**17.18**). This system was also efficient for the azidation of ibuprofen methyl ester, where azidation selectively occurred at the secondary benzylic position (**17.19**).

A plausible mechanism for this reaction commences with the visible-light excitation of the photocatalyst resulting in the formation of its triplet state **A**. Oxygen-centered radical of **A** performs HAT from a C(sp^3)–H site of the substrate **17.15**, thus producing radical **C** and ketyl radical **B**. Potentially, the HAT step could also be executed by the azide radical, which is formed upon anodic oxidation of sodium azide. Meanwhile, Mn(II) species **D** coordinates to the azide anion, forming complex **E**, which is oxidized at the anode to give Mn(III) intermediate **F**. Azide transfer from the intermediate **F** to the radical **C** delivers product **17.16** and recovers the Mn(II) catalyst. The photocatalyst is regenerated via anodic oxidation of ketyl radical **B** with loss of a proton.

Another valuable transformation, enabled by functionalized anthraquinone/cobalt tandem catalysis, was disclosed by Huang and co-workers in 2021 (Scheme 18).[38]

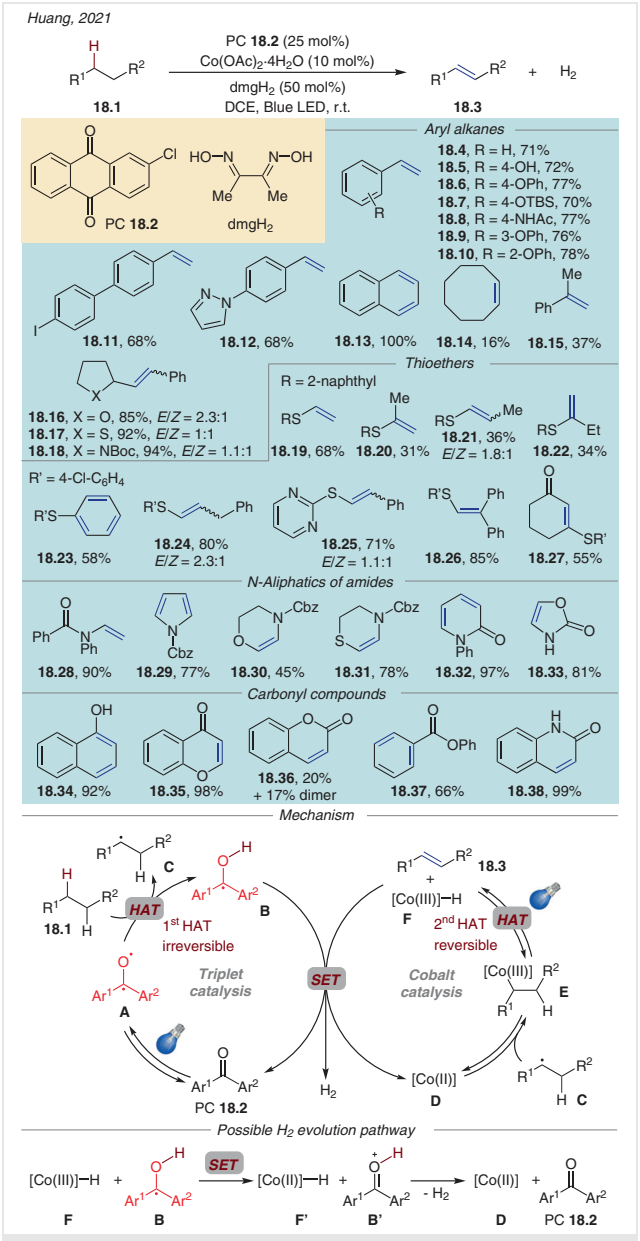

Scheme 18 Site-selective acceptorless dehydrogenation of aliphatics

The authors achieved site-selective acceptorless dehydrogenation of aliphatics in the presence of catalytic cobaloxime and 2-chloroanthraquinone (**18.3**) under blue light irradiation. The scope of this reaction proved to be very broad. Styrenes bearing unprotected hydroxy group (**18.5**), differently positioned ethers (**18.6**, **18.9**, **18.10**), silyl ether (**18.7**), amide (**18.8**), aryl iodide (**18.11**), and *N*-containing heteroarenes (**18.12**) were obtained in 68–78% yields using this protocol. Tetrahydronaphthalene afforded naphthalene quantitatively upon a double dehydrogenation reaction (**18.13**). Cyclooctane was dehydrogenated with diminished efficiency (**18.14**). Nonetheless, this example shows the applicability of this method for the desaturation of simple alkanes. Cumene afforded product **18.15** in moderate yield only. β-Substituted styrenes with heterocyclic moieties, such as furan, thiophene, and pyrrole, were obtained in high yields (**18.16**–**18.18**).

Desaturation of thioethers proceeded with varied yields (**18.19**–**18.22**). Triple dehydrogenation was achieved for cyclohexyl-containing thioether (**18.23**). Desaturation of the thioether possessing a benzylic C–H site led to alkenyl sulfide (**18.24**) over the corresponding styrene. Disubstituted (**18.25**) and trisubstituted (**18.26**) alkenes and cyclic α,β-unsaturated carbonyls (**18.27**) were obtained in moderate to good yields from the corresponding thioethers.

Amides were also successfully employed in this dehydrogenation protocol, thus representing an acceptorless desaturation of amides to enamides. Thus, an acyclic tertiary amide underwent desaturation smoothly, providing **18.28** in 90% yield. Upon double desaturation, carbazole-protected pyrrolidine delivered pyrrole **18.29**. Protected morpholine and thiomorpholine afforded desaturated products **18.30** and **18.31**, respectively. In addition, a six-membered lactam and a five-membered urethane moiety delivered products **18.32** and **18.33**.

A range of benzo-fused and acyclic ketones also underwent dehydrogenation (**18.34**–**18.37**), whilst a benzo-fused cyclic amide was desaturated in nearly quantitative yield (**18.38**).

The proposed mechanism implies two HAT events. The first irreversible HAT occurs between triplet photocatalyst **A** and the C(sp^3)–H site of **18.1**, producing carbon-centered radical **C** and ketyl radical **B**. Radical **C** then adds to cobaloxime **D** to afford Co(III)–alkyl species **E**. The latter, upon light irradiation, undergoes homolysis of the Co–C bond and a subsequent reversible cobalt-mediated β-H-atom abstraction to furnish dehydrogenated product **18.3** and Co(III) hydride **F**. Radical **B** reduces species **F** to afford Co(II)–H entity **F′** and protonated ketone **B′**, which is acidic enough to protonate Co(II)–H to release dihydrogen and regenerate the ketone and cobalt catalysts.

3 Triplet Ketone Catalysis via Single-Electron Transfer

As mentioned in the introduction section, the oxidative abilities of triplet ketones grant their applicability as oxidants in SET events with substrates or other reaction intermediates. Thus, in 2016, Murakami introduced light-excited thioxanthone (**TX**) acting as a SET agent in nickel-catalyzed homocoupling of aryl halides (Scheme 19).[39]

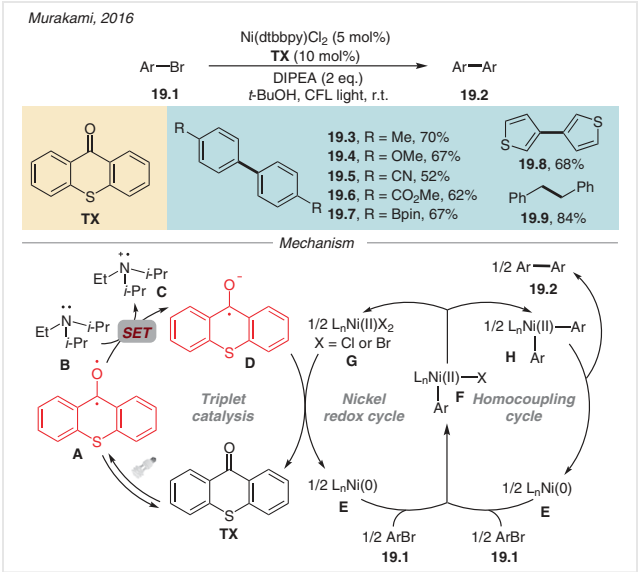

Scheme 19 Homocoupling of aryl halides

Both electron-poor and electron-rich aryl bromides performed in this transformation with equal efficiency (**19.3**–**19.7**). 3-Bromothiophene underwent homocoupling smoothly, providing product **19.8** in 68% yield. Benzyl bromide was also a suitable substrate, giving bibenzyl **19.9** in good yield.

A mechanism consisting of three catalytic cycles was proposed for this transformation. In the photocatalytic cycle, **TX** is excited by light and is converted into its triplet state **A**, which is reduced via SET from *N*,*N*-diisopropylethylamine (DIPEA) to give ketyl radical anion **D**. The latter reduces half an equivalent of Ni(II) species **G** to give half an equivalent of Ni(0) catalyst **E**, thereby regenerating **TX**. The second catalytic cycle starts with oxidative addition of aryl bromide **19.1** to Ni(0) to form arylnickel(II) entity **F**, that gives rise to nickel(II) dibromide **G** (0.5 eq.) and diarylnickel(II) **H** (0.5 eq.). The former, as mentioned above, is reduced by the radical anion **D**, while the intermediate **H** in the third cycle upon reductive elimination liberates the reaction product **19.2** and Ni(0) catalyst **E**.

In 2020, Li's group disclosed the synthesis of ketones via decarboxylative coupling of α-keto acids with aryl halides by employing CFL-induced triplet ketone/Ni catalysis (Scheme 20).[40]

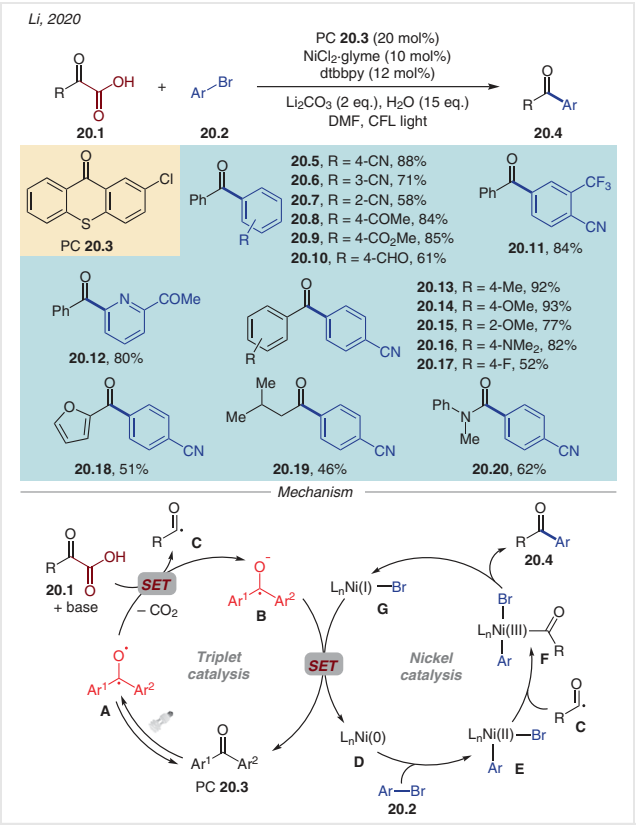

Scheme 20 Acyl radicals from α-keto acids for ketones synthesis

Series of electron-poor aryl and heteroaryl bromides reacted well with 2-oxo-2-phenylacetic acid, providing the corresponding products in good yields (**20.5**–**20.12**). However, this protocol appeared to be sensitive to the steric environment, as *ortho*-substituted aryl bromide (**20.7**) was less efficient than its *meta*- and *para*-substituted counterparts (**20.5**, **20.6**). Among the keto acids tested, electron-rich and electron-neutral phenylglyoxylic acids reacted smoothly with 4-bromobenzonitrile, delivering products **20.13**–**20.16** in high yields. A heteroaromatic α-oxo acid delivered the desired product in a moderate yield (**20.18**). The employment of an aliphatic keto acid and an oxalate monoamide led to arylation products in good yields (**20.19**, **20.20**).

A plausible reaction mechanism starts with an SET oxidation of **20.1** by triplet photocatalyst **A** to form ketyl radical anion **B** and an unstable carboxylate radical, which quickly undergoes decarboxylation to form acyl radical **C**. Meanwhile, aryl bromide **20.2** adds to the Ni(0) catalyst **D** through oxidative addition to afford Ni(II) complex **E**, which traps acyl radical **C**. The resulting Ni(III) complex **F** upon reductive elimination extrudes the product **20.4** and Ni(I) bromide species **G**. A subsequent reduction of the latter by ketyl radical anion **B** regenerates the catalysts for both cycles.

In 2021, Vincent reported the use of a 1,2-dimethylethylenediamine (DMEDA)-copper-benzophenone complex **21.3** as a multitask photocatalyst to achieve alkylation of α-amino C(sp^3)–H bonds of anilines with electron-deficient alkenes (Scheme 21).[41] This UVA-light-induced transformation required no additives.

Various Michael acceptors, including acrylates, acrylamides, enals, and 4-vinylpyridine, reacted well with *N*,*N*-dimethylaniline to provide the corresponding products in good yields (**21.5**–**21.8**). A number of electron-deficient and electron-rich tertiary anilines (**21.9**–**21.13**), secondary anilines (**21.16**–**21.18**), and aminopyridines (**21.14**, **21.15**), were capable substrates in this alkylation reaction, furnishing the desired products in good to excellent yields.

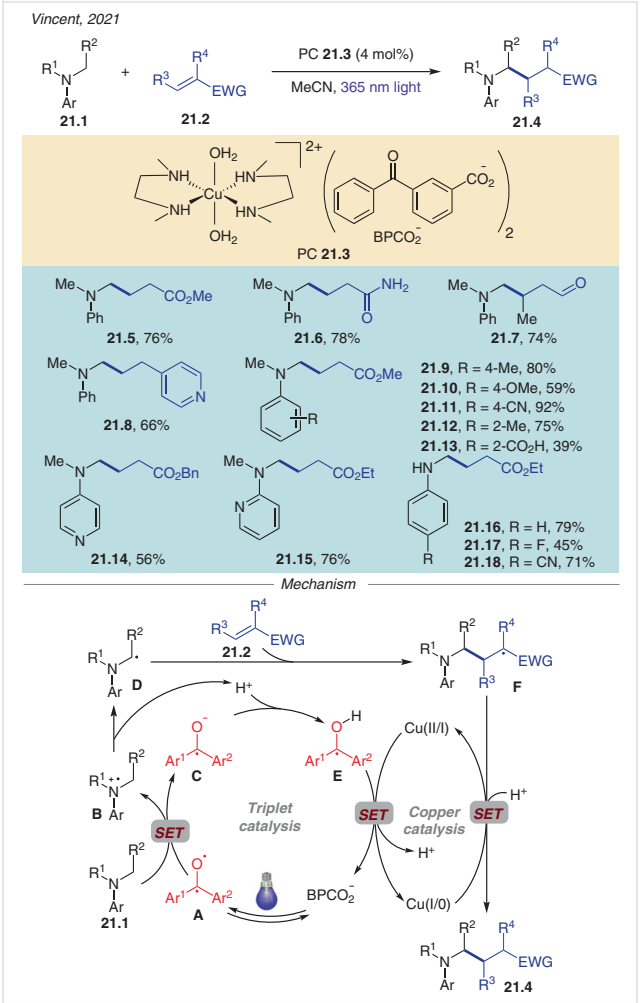

Scheme 21 Alkylation of the α-amino C–H bonds of anilines

According to the proposed mechanism, the UVA light excitation of $BPCO_2^-$ results in the formation of its triplet state **A** (E^*_{red} = 1.28 V vs SCE for benzophenone), which oxidizes aniline (E_{ox} = 1.12 vs SCE in MeCN for 4-cyano-*N*,*N*-dimethylaniline) to the radical cation **B**, while being re-

duced to a ketyl radical dianion **C**. A subsequent proton transfer from aniline radical cation **B** to species **C** results in the formation of radical **D** and a ketyl radical **E**. The former adds to Michael acceptor **21.2** to afford electrophilic alkyl radical **F**, which quickly reacts with the electron-rich Cu(I) or Cu(0) species, obtained by reduction with ketyl radical **E**. A subsequent protonation of **F** delivers the reaction product **21.4**.

In the same year, Li developed a protocol for C–P coupling between aryl halides and H-phosphine oxides or H-phosphites (Scheme 22).[42] The combination of thioxanthone and Ni/dtbby catalysts under CFL-light irradiation enabled the formation of arylphosphine oxides and arylphosphonates.

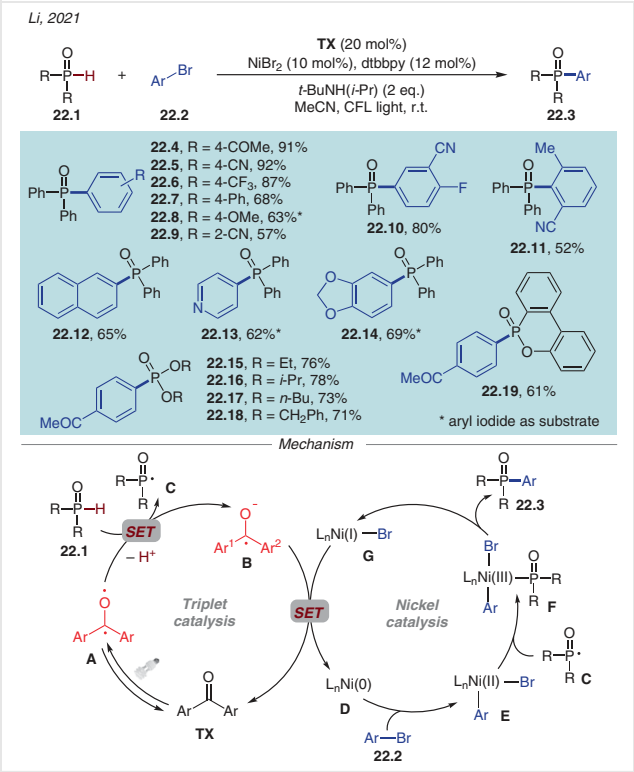

Scheme 22 P(O)–C(sp^2) coupling

Electron-deficient substrates with acetyl, cyano, or trifluoromethyl groups at the *para* position afforded products of phosphonylation with diphenylphosphine oxide in excellent yields (**22.4**–**22.6**). Phosphonylation of electron-rich aryl halides required employment of aryl iodides instead of aryl bromides (**22.8**). The reaction was less efficient with bulky aryl bromides (**22.9**, **22.11**). Napththyl and pyridyl halides delivered products in good yields (**22.12**, **22.13**), whilst dialkyl phosphites reacted well with 4′-bromoacetophenone to produce **22.15**–**22.18** in good yields.

The reaction mechanism commences with SET between triplet thioxanthone **A** and H-phosphine oxide (H-phosphite) **22.1**, resulting in formation of *P*-centered radical **C** and ketyl radical anion **B**. The high reduction potential of triplet thioxanthone ($E(\mathbf{TX}^*/\mathbf{TX}^{\bullet-})$ = 1.34 V vs SCE in DMF)[43] is sufficient to oxidize the H-phosphine oxide or H-phosphite with E_{ox} ≈ 1.0 V vs SCE. Concurrently, the Ni(0) catalyst undergoes oxidative addition with the aryl bromide to yield Ni(II) complex **E**, which intercepts radical **C** to produce Ni(III) species **F**. The latter delivers functionalized product **22.3** and Ni(I) bromide **G** upon reductive elimination. Ni(I) bromide **G** is reduced by ketyl radical anion **B**, returning the Ni(0) and **TX** catalysts to the cycle.

A year later, the same group reported a C–S cross-coupling reaction between aryl halides and sodium sulfinates, operating via an identical mechanism (Scheme 23).[43]

The photocatalyst chosen for this transformation (**23.3**) had a high excited-state reduction potential of 1.47 V vs SCE in DMF, which was essential for the success of the reaction. Accordingly, the employment of thioxanthone with a lower excited-state reduction potential (1.34 V vs SCE in DMF) provided products in diminished yields.

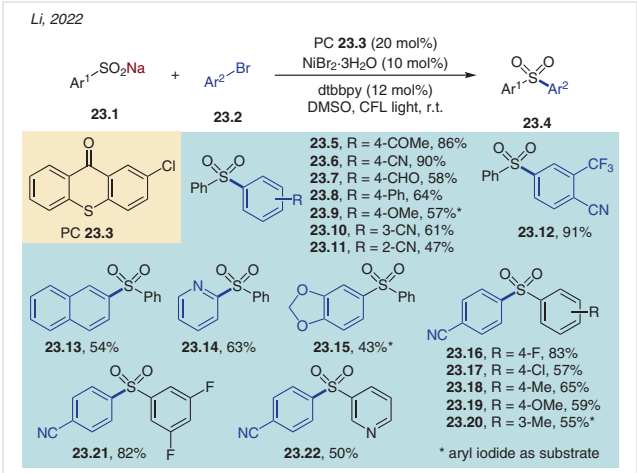

Scheme 23 Cross-coupling of aryl halides with sodium sulfinates

The scope of this transformation with respect to aryl bromides is analogous to that for their C–P coupling protocol.[42] The yields of coupled products were also somewhat diminished for electron-rich or sterically hindered aryl bromides (**23.9**, **23.11**).

The scope of aryl sulfinates is quite general, as electronically diverse substrates led to products in moderate to good yields (**23.16**–**23.22**).

4 Triplet Ketone Catalysis via Energy Transfer

In 2017, Xiao's group revealed a method for the asymmetric aerobic oxidation of β-ketoesters (Scheme 24).[44] In this protocol, the authors developed a new visible-light-responsive ligand **24.2** consisting of a chiral bisoxazoline (BOX) moiety **24.4** and a thioxanthone motif **24.5** attached

to BOX through an esterification reaction. Ligand **24.2** upon complexation with Ni(acac) leads to a chiral photocatalyst, enabling visible-light-induced aerobic oxidation of β-ketoesters.

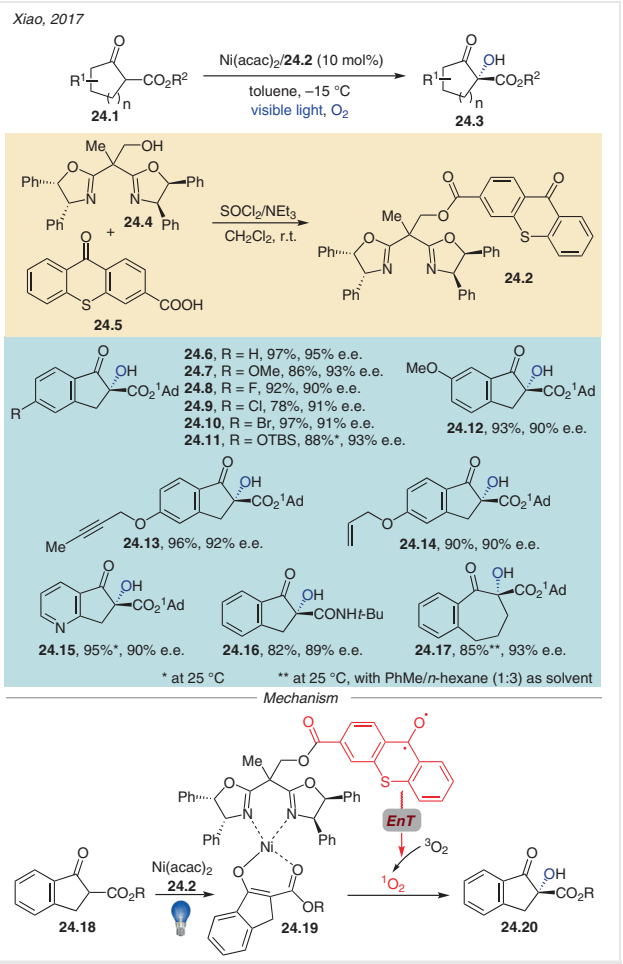

Scheme 24 Enantioselective aerobic oxidation of β-ketoesters

1-Indanone derivatives bearing various substituents on the aromatic ring performed nicely, affording products **24.6**–**24.12** in excellent yields with 90–95% e.e. Notably, hydroxylation of substrates with sensitive to oxidation moieties, such as double or triple bonds, or heteroaryls, proceeded uneventfully delivering products **24.13**–**24.15** without a drop in the yield or enantioselectivity. Substrates with an amide group (**24.16**) or a seven-membered bicyclic β-ketoester (**24.17**) were also compatible with these reaction conditions.

This reaction starts with *in situ* generation of the bifunctional chiral catalyst (**24.18** → **24.19**). Upon visible-light excitation, the thioxanthone part of the catalyst converts into its triplet state, which transfers energy to the unreactive triplet state of molecular oxygen ($^3O_2$). The generated reactive singlet oxygen species oxidizes the enolate form of the substrate to give α-hydroxy β-ketoester **24.20**.

In 2019, Li disclosed thioxanthone/nickel-photocatalyzed esterification of carboxylic acids with aryl bromides (Scheme 25).[45] Light-excited thioxanthone in this system acts as a photosensitizer, thus significantly accelerating the transformation. Notably, this protocol represents an organic photocatalyst/Ni version of MacMillan's Ir/Ni dual photocatalytic system.[46]

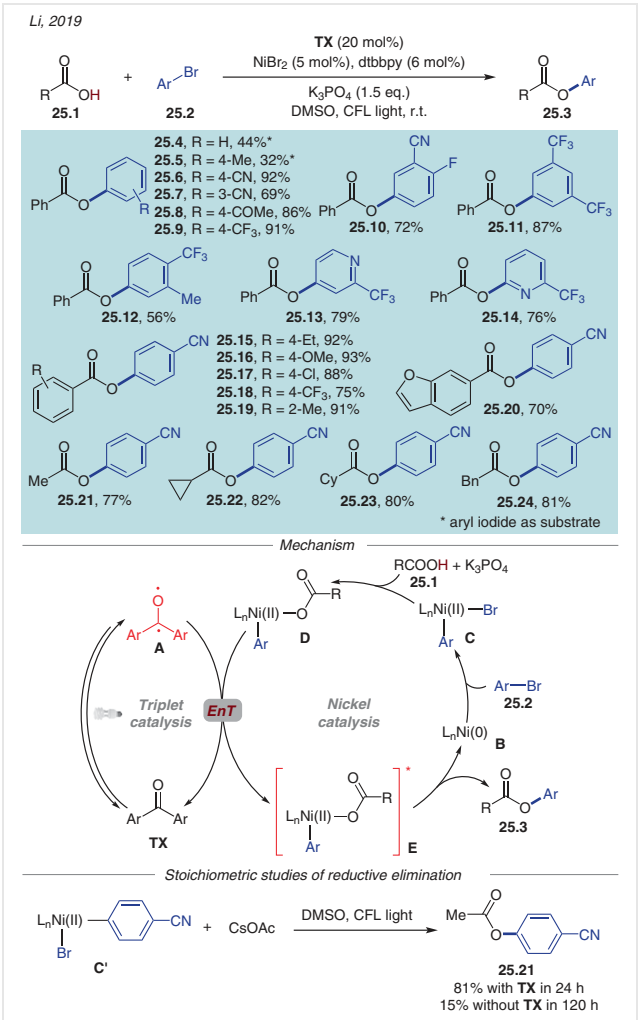

Scheme 25 Aryl esterification

Under standard reaction conditions, aryl bromides bearing electron-withdrawing substituents smoothly coupled with benzoic acid, providing products **25.6**–**25.11** in good to excellent yields. The combination of 4-CF_3 and 3-methyl substitution also worked well (**25.12**). Although bromobenzene and 1-bromo-4-methylbenzene were not reactive, their iodo analogs were competent reaction partners (**25.4**, **25.5**). Substituted pyridine-based heteroaryl bromides

were also suitable coupling partners (**25.13**, **25.14**). The scope of carboxylic acids for this transformation is quite broad, as benzoic acids with alkyl, alkoxy, halide, and trifluoromethyl substituents on the aromatic ring were efficient substrates (**25.15**–**25.19**). Likewise, other acyclic and cyclic carboxylic acids reacted well, delivering products **25.20**–**25.24** in good yields.

This reaction operates via a similar mechanism to that established by MacMillan et al. for their dual Ir/Ni photocatalytic system for esterification.[46] Aryl bromide **25.2** oxidatively adds to the ligated Ni(0) catalyst **B**, affording Ni(II) species **C**, which undergoes ligand exchange with carboxylate nucleophile **25.1** to yield Ar–Ni(II)–carboxylate **D**. Excited triplet **A** upon triplet–triplet energy transfer to **D** generates excited-state complex **E** and recovers **TX**. The excited-state complex **E** then undergoes reductive elimination to afford reaction product **25.3** and the active Ni(0) catalyst.

Later, the same group demonstrated visible-light-induced nickel-catalyzed Sonogashira coupling (Scheme 26).[47] The key reaction catalyst, along with Ni(0)/dtbbpy, was again thioxanthone, performing energy transfer after the excited state formation with CFL light. Thioxanthone, with the highest triplet state energy of 63.4 kcal/mol, performed the most efficiently in comparison with other photocatalysts.

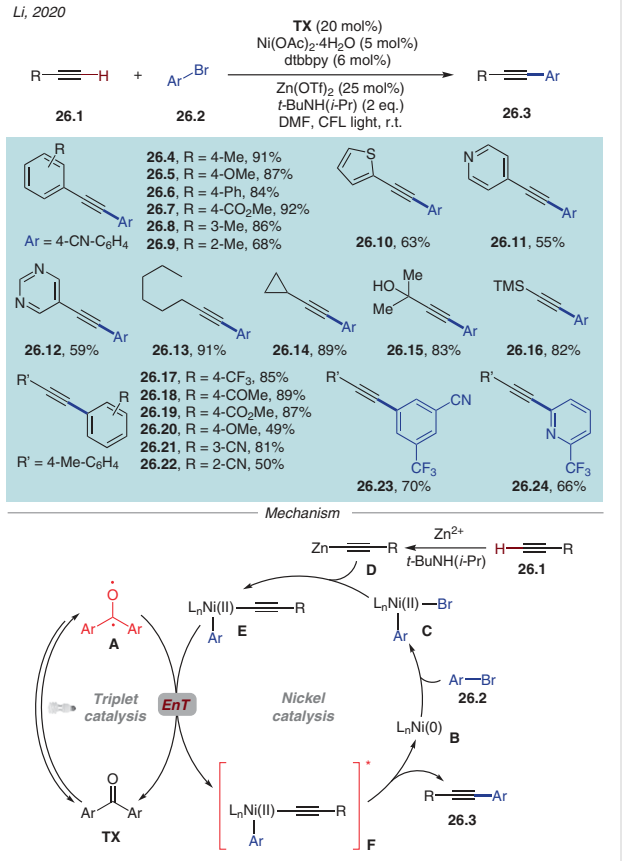

Scheme 26 Sonogashira C(sp)–C(sp^2) coupling

Electronically different aryl alkynes were effective coupling partners (**26.4**–**26.7**). However, the use of substrates with *meta* and *ortho* substituents resulted in slightly decreased yields (**26.8**, **26.9**). Heteroaryl alkynes proved compatible with the reaction protocol, affording coupling products **26.10**–**26.12** in moderate yields. Primary, secondary, hydroxy-substituted, and silane-substituted alkyls were transformed into coupling products smoothly (**26.13**–**26.16**). Electron-poor aryl bromides (**26.17**–**26.19**, **26.21**, **26.23**) provided notably higher yields than their electron-rich analog **26.20**.

This cross-coupling reaction starts with oxidative addition of aryl bromide **26.2** to Ni(0), yielding arylnickel(II) bromide **C**, which undergoes transmetalation with Zn(II) acetylide **D** to form Ar–Ni(II)–acetylide **E**. Concomitantly, visible light converts the **TX** photocatalyst into its triplet state **A**, which transfers energy to complex **E** via a triplet–triplet energy transfer path. Upon this process, complex **E** converts into its excited state **F**, whereas **TX** returns to its ground state. Finally, reductive elimination from intermediate **F** liberates the product **26.3** and returns Ni(0) to the cycle.

Another contribution of Li's group in the field of dual triplet ketone/metal catalysis is the **TX**/nickel-catalyzed etherification of phenols and aryl halides (Scheme 27).[48] This reaction follows a mechanistic pathway similar to those described above.[41–43]

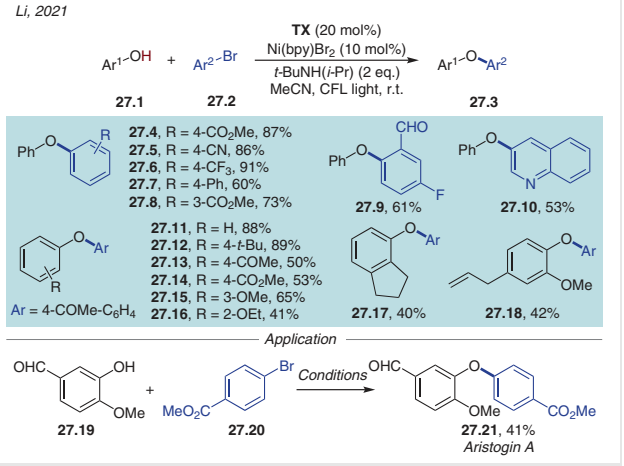

Scheme 27 Etherification of phenols and aryl halides

In this transformation, electron-poor aryl bromides were mostly employed. Thus, ester, nitrile, trifluoromethyl, phenyl, aldehyde, and fluorine moieties were compatible with the reaction protocol, delivering etherification products of phenol **27.4**–**27.9** in moderate to good yields. 3-Bromoquinoline also reacted smoothly, furnishing product **27.10** in 53% yield.

Different phenols were tested in the etherification reaction with 1-(4-bromophenyl)ethan-1-one. Electron-neutral and electron-rich phenols performed well (**27.11**, **27.12**), whereas electron-poor phenols were less efficient (**27.13**, **27.14**). Fused phenols and those possessing an alkene functionality were also suitable for this system (**27.17**, **27.18**).

The applicability of this protocol to the synthesis of pharmaceutically relevant products was shown by the reaction of 3-hydroxy-4-methoxybenzaldehyde (**27.19**) with methyl 4-bromobenzoate (**27.20**), which delivered the natural product aristogin A in moderate yield.

5 Conclusions

Synergistic triplet ketone/transition-metal catalysis has become an emerging area of photochemistry in recent years. It is largely attributed to the broad accessibility and useful features of light-excited carbonyls. Their ability to perform HAT, SET, and EnT in tandem with metal catalysis has enabled the development of facile functionalizations at $C(sp^3)$–H and $C(sp^2)$–H bonds. Among these transformations, alkylation, arylation, acylation, carboxylation, dehydrogenation, sulfonylation, cyanation, azidation, phosphonylation, hydroxylation, esterification, and etherification reactions, along with three-component couplings, have been developed.

Nevertheless, some challenges remain unsolved in dual triplet ketone/metal catalysis. Many reactions require harsh UVA light irradiation, which might be incompatible with substrates possessing reactive or prone to polymerization functionalities. The employment of light of lower energy is needed for the benign functionalization of such molecules. This can be achieved by tuning the electronic and photophysical properties of the ketone catalysts, aiming at moving their absorption maxima toward the red region of the spectrum. Structural modifications of a carbonyl photocatalyst may also affect its HAT ability, reduction potential, and triplet energy. Moreover, further investigation is needed to solve the reoccurring problem of deactivation of benzophenone-type photocatalysts through pinacol formation in transformations involving triplet ketones as HAT agents.

In addition, there are plentiful possibilities for discoveries in energy transfer between triplet ketones and transition-metal catalysts. Existing examples of this type of transformation are very scarce and are mostly limited to nickel catalysis. The employment of other transition metals in triplet energy transfer with ketone photosensitizers could potentially uncover new and exciting reactivities.

Conflict of Interest

The authors declare no conflict of interest.

Funding Information

We thank the National Institutes of Health (GM120281), the National Science Foundation (CHE-1955663), and the Welch Foundation (Chair, AT-0041) for financial support.

References

(1) Selected reviews: (a) Fagnoni, M.; Dondi, D.; Ravelli, D.; Albini, A. *Chem. Rev.* **2007**, *107*, 2725. (b) Ravelli, D.; Dondi, D.; Fagnoni, M.; Albini, A. *Chem. Soc. Rev.* **2009**, *38*, 1999. (c) Ravelli, D.; Fagnoni, M.; Albini, A. *Chem. Soc. Rev.* **2013**, *42*, 97. (d) Romero, N. A.; Nicewicz, D. A. *Chem. Rev.* **2016**, *116*, 10075. (e) Sideri, I. K.; Voutyritsa, E.; Kokotos, C. G. *Org. Biomol. Chem.* **2018**, *16*, 4596. (f) Dantas, J. A.; Correia, J. T. M.; Paixão, M. W.; Corrêa, A. G. *ChemPhotoChem* **2019**, *3*, 506.

(2) Elliott, L. D.; Kayal, S.; George, M. W.; Booker-Milburn, K. *J. Am. Chem. Soc.* **2020**, *142*, 14947.

(3) Hassan, M. M.; Olaoye, O. O. *Molecules* **2020**, *25*, 2285.

(4) Turro, N. J.; Ramamurthy, V.; Ramamurthy, V.; Scaiano, J. C. In *Principles of Molecular Photochemistry: An Introduction*; Stiefel, J., Ed.; University Science Books: Sausalito, **2009**, 231.

(5) Wagner, P. J. *Top. Curr. Chem.* **1976**, *66*, 1.

(6) Selected reviews: (a) Capaldo, L.; Ravelli, D. *Eur. J. Org. Chem.* **2017**, 2056. (b) Ye, Z.; Lin, Y.-M.; Gong, L. *Eur. J. Org. Chem.* **2021**, 5545. (c) Cao, H.; Tang, X.; Tang, H.; Yuan, Y.; Wu, J. *Chem Catal.* **2021**, *1*, 523. (d) Gkizis, P. L. *Eur. J. Org. Chem.* **2022**, e202201139. (e) Capaldo, L.; Ravelli, D.; Fagnoni, M. *Chem. Rev.* **2022**, *122*, 1875. (f) Holmberg-Douglas, N.; Nicewicz, D. A. *Chem. Rev.* **2022**, *122*, 1925. (g) Golden, D. L.; Suh, S.-E.; Stahl, S. S. *Nat. Rev. Chem.* **2022**, *6*, 405.

(7) Fujiya, A.; Nobuta, T.; Yamaguchi, E.; Tada, N.; Miura, T.; Itoh, A. *RSC Adv.* **2015**, *5*, 39539.

(8) (a) Schaefer, C. G.; Peters, K. S. *J. Am. Chem. Soc.* **1980**, *102*, 7566. (b) Yamashita, T.; Yasuda, M.; Watanabe, M.; Kojima, R.; Tanabe, K.; Shima, K. *J. Org. Chem.* **1996**, *61*, 6438. (c) Bertrand, S.; Glapski, C.; Hoffmann, N.; Pete, J.-P. *Tetrahedron Lett.* **1999**, *40*, 3169. (d) Harakat, D.; Pesch, J.; Marinkovic, S.; Hoffmann, N. *Org. Biomol. Chem.* **2006**, *4*, 1202. (e) Hoffmann, N. *Synthesis* **2016**, *48*, 1782. (f) Li, L.; Mu, X.; Liu, W.; Wang, Y.; Mi, Z.; Li, C.-J. *J. Am. Chem. Soc.* **2016**, *138*, 5809. (g) Tripathi, C. B.; Ohtani, T.; Corbett, M. T.; Ooi, T. *Chem. Sci.* **2017**, *8*, 5622. (h) Cervantes-González, J.; Vosburg, D. A.; Mora-Rodriguez, S. E.; Vázquez, M. A.; Zepeda, L. G.; Villegas Gómez, C.; Lagunas-Rivera, S. *ChemCatChem* **2020**, *12*, 3811.

(9) (a) Leigh, W. J.; Arnold, D. R.; Humphreys, R. W. R.; Wong, P. C. *Can. J. Chem.* **1980**, *58*, 2537. (b) Timpe, H.-J.; Kronfeld, K.-P. J. *Photochem. Photobiol. A* **1989**, *46*, 253.

(10) (a) Albini, A. *Synthesis* **1981**, 249. (b) Perez-Prieto, J.; Galian, R. E.; Miranda, M. A. *Mini Rev. Org. Chem.* **2006**, *3*, 117. (c) Tröster, A.; Alonso, R.; Bauer, A.; Bach, T. *J. Am. Chem. Soc.* **2016**, *138*, 7808. (d) Poplata, S.; Tröster, A.; Zou, Y.-Q.; Bach, T. *Chem. Rev.* **2016**, *116*, 9748. (e) Iyer, A.; Clay, A.; Jockusch, S.; Sivaguru, J. *J. Phys. Org. Chem.* **2017**, *30*, e3738. (f) Neveselý, T.; Daniliuc, C. G.; Gilmour, R. *Org. Lett.* **2019**, *21*, 9724. (g) Strieth-Kalthoff, F.; Glorius, F. *Chem* **2020**, *6*, 1888.

(11) Aloïse, S.; Ruckebusch, C.; Blanchet, L.; Réhault, J.; Buntinx, G.; Huvenne, J.-P. *J. Phys. Chem. A* **2008**, *112*, 224.

(12) (a) Kearns, D. R.; Case, W. A. *J. Am. Chem. Soc.* **1966**, *88*, 5087. (b) Arnold, D. R. *Adv. Photochem.* **1968**, *6*, 301. (c) Strieth-Kalthoff, F.; James, M. J.; Teders, M.; Pitzer, L.; Glorius, F. *Chem. Soc. Rev.* **2018**, *47*, 7190.

(13) Zhu, D. L.; Young, D. J.; Li, H. X. *Synthesis* **2020**, *52*, 3493.
(14) Chow, Y. L.; Buono-Core, G. E.; Lee, C. W.; Scaiano, J. C. *J. Am. Chem. Soc.* **1986**, *108*, 7620.
(15) Almansa, A.; Jardel, D.; Massip, S.; Tassaing, T.; Schatz, C.; Domergue, J.; Molton, F.; Duboc, C.; Vincent, J.-M. *J. Org. Chem.* **2022**, *87*, 11172.
(16) Shen, Y.; Gu, Y.; Martin, R. *J. Am. Chem. Soc.* **2018**, *140*, 12200.
(17) (a) Börjesson, M.; Moragas, T.; Martin, R. *J. Am. Chem. Soc.* **2016**, *138*, 7504. (b) Terrett, J. A.; Cuthbertson, J. D.; Shurtleff, V. W.; MacMillan, D. W. C. *Nature* **2015**, *524*, 330.
(18) Bonciolini, S.; Noël, T.; Capaldo, L. *Eur. J. Org. Chem.* **2022**, e202200417.
(19) Xue, X.-S.; Ji, P.; Zhou, B.; Cheng, J.-P. *Chem. Rev.* **2017**, *117*, 8622.
(20) Dewanji, A.; Krach, P. E.; Rueping, M. *Angew. Chem. Int. Ed.* **2019**, *58*, 3566.
(21) Sanjose-Orduna, J.; Silva, R. C.; Raymenants, F.; Reus, B.; Thaens, J.; de Oliveira, K. T.; Noël, T. *Chem. Sci.* **2022**, *13*, 12527.
(22) Krach, P. E.; Dewanji, A.; Yuan, T.; Rueping, M. *Chem. Commun.* **2020**, *56*, 6082.
(23) Ren, C.-C.; Wang, T.-Q.; Zhang, Y.; Peng, D.; Liu, X.-Q.; Wu, Q.-A.; Liu, X.-F.; Luo, S.-P. *ChemistrySelect* **2021**, *6*, 2523.
(24) Schirmer, T. E.; Wimmer, A.; Weinzierl, F. W. C.; König, B. *Chem. Commun.* **2019**, *55*, 10796.
(25) Ishida, N.; Masuda, Y.; Imamura, Y.; Yamazaki, K.; Murakami, M. *J. Am. Chem. Soc.* **2019**, *141*, 19611.
(26) Cao, S.; Hong, W.; Ye, Z.; Gong, L. *Nat. Commun.* **2021**, *12*, 2377.
(27) Campbell, M. W.; Yuan, M.; Polites, V. C.; Gutierrez, O.; Molander, G. A. *J. Am. Chem. Soc.* **2021**, *143*, 3901.
(28) Viehe, H. G.; Janousek, Z.; Merenyi, R.; Stella, L. *Acc. Chem. Res.* **1985**, *18*, 148.
(29) Luridiana, A.; Mazzarella, D.; Capaldo, L.; Rincon, J. A.; Garcia-Losada, P.; Mateos, C.; Frederick, M. O.; Nuno, M.; Jan Buma, W.; Noël, T. *ACS Catal.* **2022**, *12*, 11216.
(30) Ishida, N.; Masuda, Y.; Uemoto, S.; Murakami, M. *Chem. Eur. J.* **2016**, *22*, 6524.
(31) Abadie, B.; Jardel, D.; Pozzi, G.; Toullec, P.; Vincent, J.-M. *Chem. Eur. J.* **2019**, *25*, 16120.
(32) Li, Y. J.; Lei, M.; Gong, L. *Nat. Catal.* **2019**, *2*, 1016.
(33) Zhang, S.; Cao, S.; Lin, Y.-M.; Sha, L.; Lu, C.; Gong, L. *Chin. J. Catal.* **2022**, *43*, 564.
(34) Fan, W.; Zhao, X.; Deng, Y.; Chen, P.; Wang, F.; Liu, G. *J. Am. Chem. Soc.* **2022**, *144*, 21674.
(35) Zhang, W.; Wang, F.; McCann, S. D.; Wang, D.; Chen, P.; Stahl, S. S.; Liu, G. *Science* **2016**, *353*, 1014.
(36) Wang, L.; Wang, T.; Cheng, G.-J.; Li, X.; Wei, J.-J.; Guo, B.; Zheng, C.; Chen, G.; Ran, C.; Zheng, C. *ACS Catal.* **2020**, *10*, 7543.
(37) Niu, L.; Jiang, C.; Liang, Y.; Liu, D.; Bu, F.; Shi, R.; Chen, H.; Chowdhury, A. D.; Lei, A. *J. Am. Chem. Soc.* **2020**, *142*, 17693.
(38) Zhou, M. J.; Zhang, L.; Liu, G.; Xu, C.; Huang, Z. *J. Am. Chem. Soc.* **2021**, *143*, 16470.
(39) Masuda, Y.; Ishida, N.; Murakami, M. *Eur. J. Org. Chem.* **2016**, 5822.
(40) Zhu, D.-L.; Wu, Q.; Young, D. J.; Wang, H.; Ren, Z.-G.; Li, H.-X. *Org. Lett.* **2020**, *22*, 6832.
(41) Abadie, B.; Jonusauskas, G.; McClenaghan, N. D.; Toullec, P. Y.; Vincent, J.-M. *Org. Biomol. Chem.* **2021**, *19*, 5800.
(42) Zhu, D.-L.; Jiang, S.; Wu, Q.; Wang, H.; Chai, L.-L.; Li, H.-Y.; Li, H.-X. *Org. Lett.* **2021**, *23*, 160.
(43) Jiang, S.; Zhang, Z.-T.; Young, D. J.; Chai, L.-L.; Wu, Q.; Li, H.-X. *Org. Chem. Front.* **2022**, *9*, 1437.
(44) Ding, W.; Lu, L. Q.; Zhou, Q. Q.; Wei, Y.; Chen, J. R.; Xiao, W. J. *J. Am. Chem. Soc.* **2017**, *139*, 63.
(45) Zhu, D.-L.; Li, H.-X.; Xu, Z.-M.; Li, H.-Y.; Young, D. J.; Lang, J.-P. *Org. Chem. Front.* **2019**, *6*, 2353.
(46) Welin, E. R.; Le, C.; Arias-Rotondo, D. M.; McCusker, J. K.; MacMillan, D. W. C. *Science* **2017**, *355*, 380.
(47) Zhu, D.-L.; Xu, R.; Wu, Q.; Li, H.-Y.; Lang, J.-P.; Li, H.-X. *J. Org. Chem.* **2020**, *85*, 9201.
(48) Zhu, D.-L.; Jiang, S.; Wu, Q.; Wang, H.; Li, H.-Y.; Li, H.-X. *Org. Lett.* **2021**, *23*, 8327.

